UPPSALA
UNIVERSITET

Data-mining approaches to find new materials

Olle Eriksson, Department of Physics and Astronomy, Uppsala University

And

School of Science and Technology, Örebro University

Collaborators

Abrikosov, Bergman, Bergqvist, Björkman, Bluegel, Brena, Burlamaqui, Cardias, Chico, Chimata, Delczeg-Czirjak, Delin, Di Marco, Etz, Grechnev, Grånäs, Hellsvik Iusan, Johansson, Katsnelson, Kimel, Kirilyuk, Klautau, Klintenberg, Kvashnin, Koumpouros, Lichtenstein, Locht, Luder, Mentink, Nordström, Panda, Pereiro, Rodrqigues, Rasing, Rodriques, Russ, Sanyal, Szilva, Szunyogh, Thonig, Thunström, Yudin, Wills

UPPSALA UNIVERSITET

Overview

Comparing methods
An electronic-structure data-base
Finding new 2D materials
Are there more high temperature superconductors ?
A data-base for Ce compounds
Some experience with DMFT
Conclusion

Comparing methods

UPPSALA UNIVERSITET

Density functional theory

$$\left(-\frac{\nabla^2}{2} + V_{eff}\right)\psi = \varepsilon\psi$$

$$V_{eff}(n(r))$$

$$n(r) = \sum |\psi(r)|^2$$

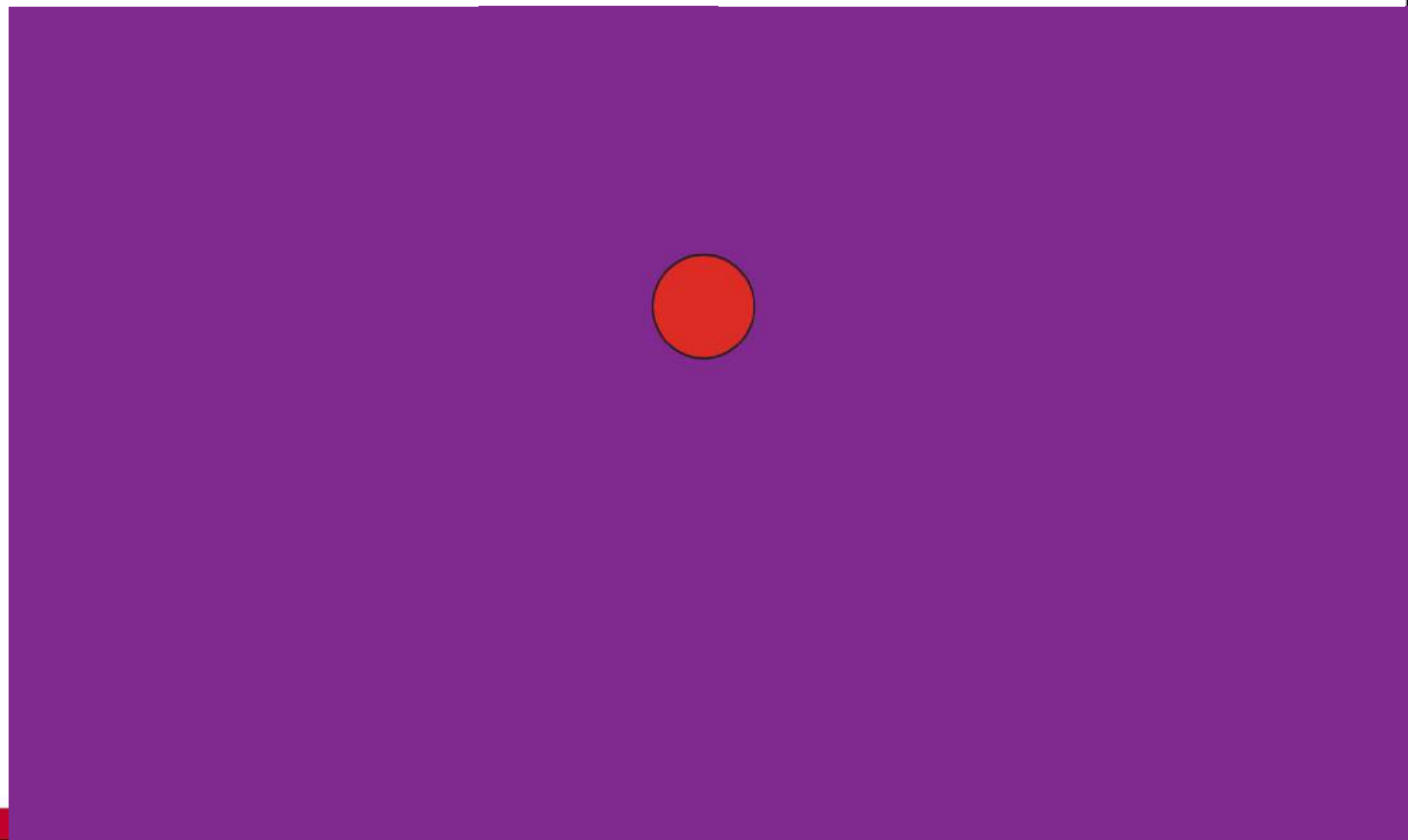

UPPSALA UNIVERSITET

FP-LMTO

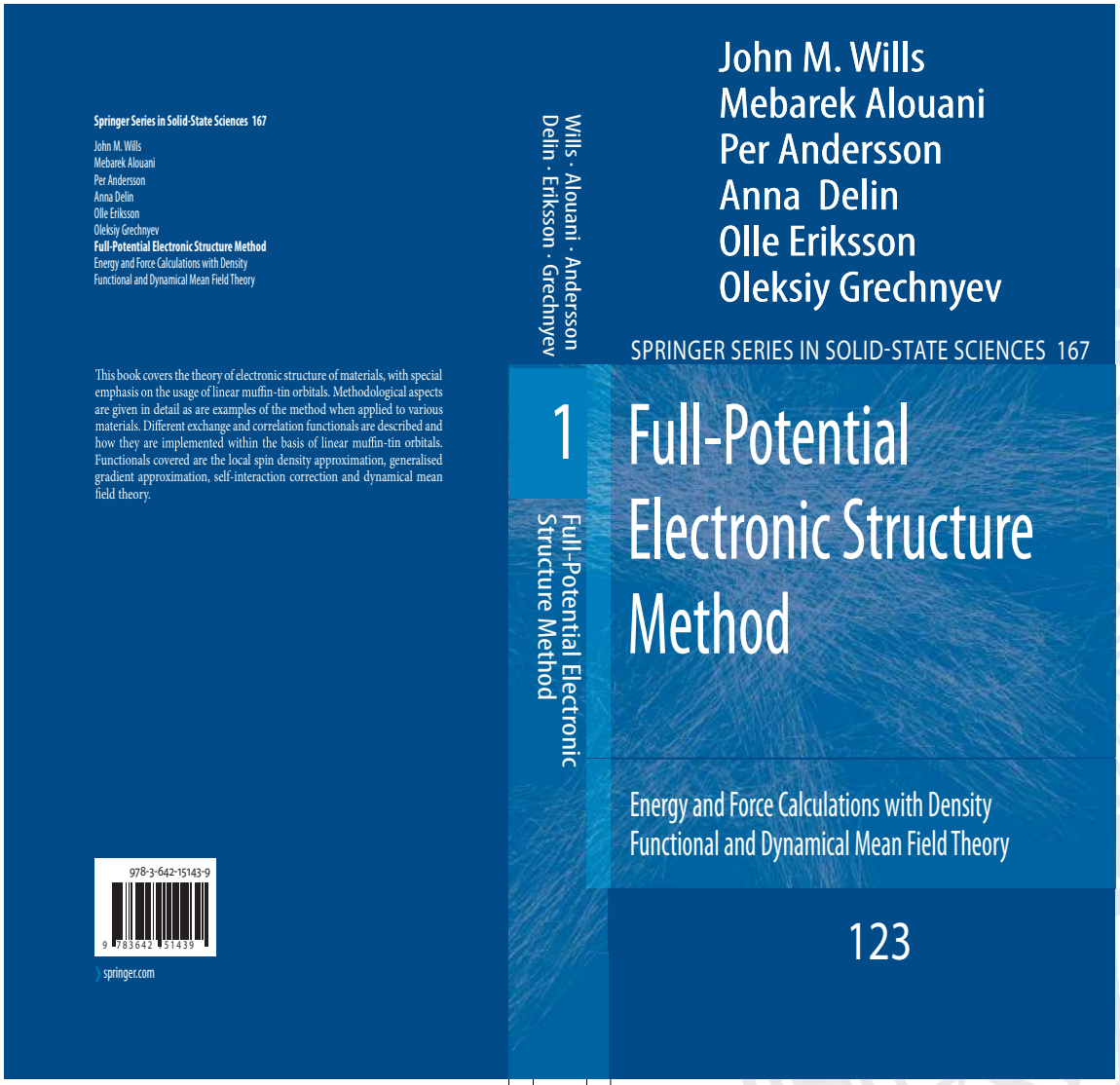

DMFT implementation:

1. Grechnev, Di Marco et al.
PRB, 76, 35107 (2007)
2. Di Marco et al
PRB 79 115111 (2009)
3. Thunström et al.
PRB 79, 165104 (2009)
4. Grånäs et al.
Comp. Mat. Sci. 55, 295 (2012)
5. Thunström, Di Marco et al.
PRL 109, 186401 (2012).

Katsnelson+Lichtenstein

UPPSALA UNIVERSITET

The delta-test setup

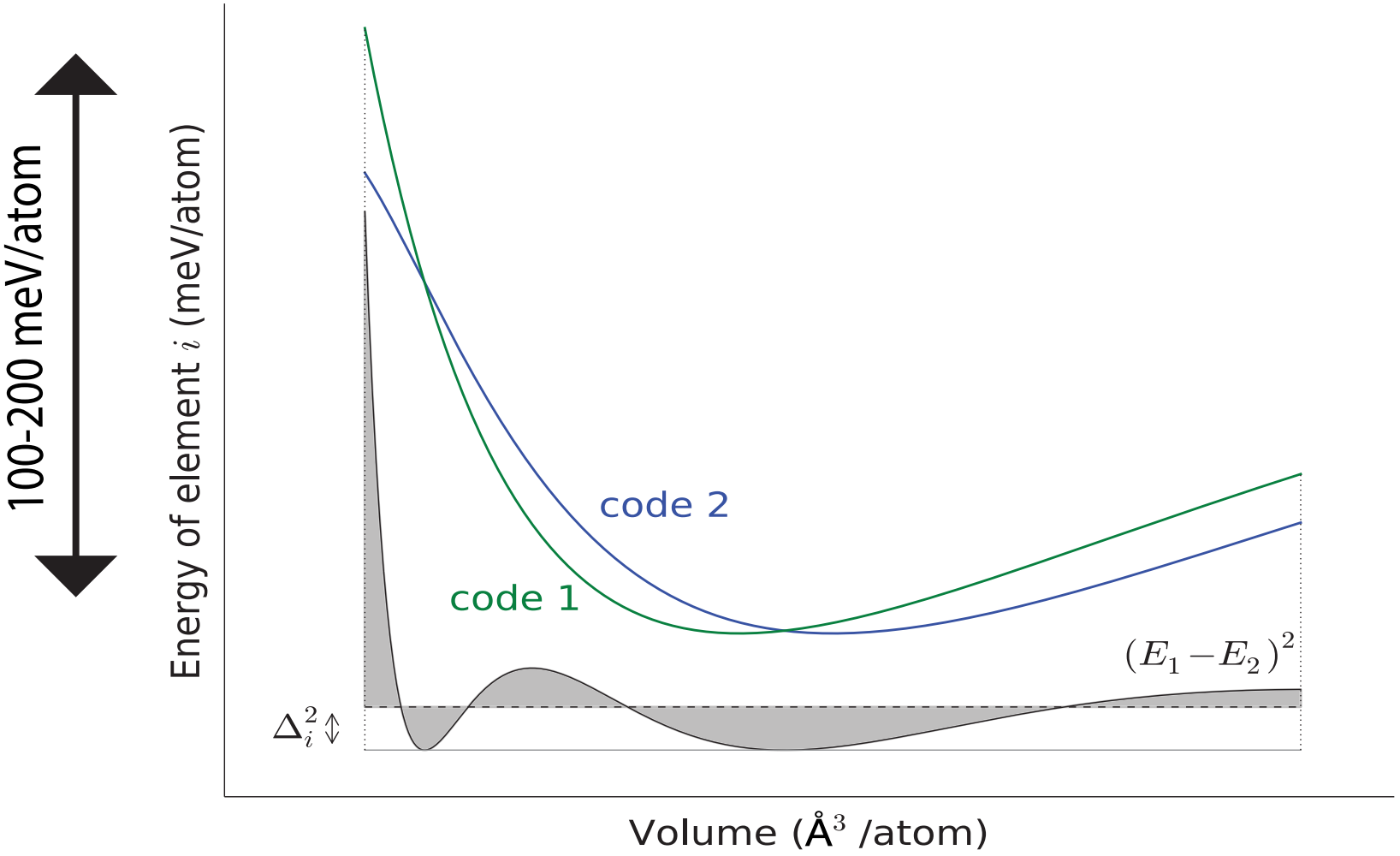

	WIEN2k-new	FLEUR	RSPt	FPLO_TplusF_soft	FPLO_TplusF	FPLO_default	Abinit_JTH2	Abinit_JTH	Abinit_delta40	GPAW09	GPAW06	QE31	VASPGW	VASP53hard	VASP52	VASP	CASTEP8	CASTEP7	CASTEP-MS	CASTEP-USP	OpenMX	DACAPO	Abinit_FHI
WIEN2k-new	0.0	0.8	0.8	0.9	1.0	3.9	0.6	1.2	1.3	1.5	3.8	1.8	0.8	0.7	1.0	2.1	0.5	2.4	3.4	7.7	2.0	6.2	14.5
FLEUR	0.8	0.0	0.7	0.9	0.9	3.5	0.7	0.8	1.5	1.7	3.4	1.6	1.2	0.9	1.3	1.8	1.0	2.8	3.7	7.8	1.7	6.5	13.8
RSPt	0.8	0.7	0.0	0.9	0.7	3.2	0.7	0.9	1.5	1.7	3.4	1.6	1.2	1.0	1.3	1.9	1.1	3.0	3.9	7.9	1.8	6.5	14.0
FPLO_TplusF_sof	0.9	0.9	0.9	0.0	0.8	3.6	0.9	1.2	1.7	1.9	3.5	1.6	1.3	1.2	1.4	1.9	1.1	2.9	3.7	7.7	1.8	6.4	13.9
FPLO_TplusF	1.0	0.9	0.7	0.8	0.0	3.1	0.9	1.0	1.8	2.0	3.4	1.6	1.3	1.1	1.5	1.9	1.2	3.1	3.9	7.9	1.8	6.4	14.6
FPLO_default	3.9	3.5	3.2	3.6	3.1	0.0	3.6	3.4	4.1	4.2	3.1	3.3	4.0	3.9	4.0	2.8	4.0	5.8	6.2	8.9	3.2	7.2	13.6
Abinit_JTH2	0.6	0.7	0.7	0.9	0.9	3.6	0.0	0.9	1.4	1.6	3.5	1.6	1.0	0.7	1.0	1.9	0.7	2.6	3.6	7.6	1.9	6.2	14.2
Abinit_JTH	1.2	0.8	0.9	1.2	1.0	3.4	0.9	0.0	1.5	1.8	3.2	1.6	1.6	1.4	1.6	1.9	1.3	3.0	3.8	7.9	1.5	6.5	13.4
Abinit_delta40	1.3	1.5	1.5	1.7	1.8	4.1	1.4	1.5	0.0	0.7	3.6	2.2	1.6	1.4	1.7	2.4	1.4	2.5	3.5	7.9	2.3	6.0	14.2
GPAW09	1.5	1.7	1.7	1.9	2.0	4.2	1.6	1.8	0.7	0.0	3.6	2.3	1.9	1.7	1.9	2.5	1.6	2.8	3.7	8.0	2.5	6.4	14.3
GPAW06	3.8	3.4	3.4	3.5	3.4	3.1	3.5	3.2	3.6	3.6	0.0	2.9	4.0	3.7	3.9	2.8	3.8	5.6	5.6	8.6	3.0	7.6	13.0
QE31	1.8	1.6	1.6	1.6	1.6	3.3	1.6	1.6	2.2	2.3	2.9	0.0	1.9	1.8	1.9	1.5	1.7	3.3	3.7	7.4	1.8	5.9	14.1
VASPGW	0.8	1.2	1.2	1.3	1.3	4.0	1.0	1.6	1.6	1.9	4.0	1.9	0.0	0.8	1.2	2.1	0.8	2.6	3.6	8.1	2.2	6.1	15.1
VASP53hard	0.7	0.9	1.0	1.2	1.1	3.9	0.7	1.4	1.4	1.7	3.7	1.8	0.8	0.0	0.5	1.8	0.8	2.6	3.5	7.8	2.1	6.3	14.5
VASP52	1.0	1.3	1.3	1.4	1.5	4.0	1.0	1.6	1.7	1.9	3.9	1.9	1.2	0.5	0.0	1.7	1.0	2.8	3.8	8.0	2.3	6.8	14.5
VASP	2.1	1.8	1.9	1.9	1.9	2.8	1.9	1.9	2.4	2.5	2.8	1.5	2.1	1.8	1.7	0.0	2.1	3.5	4.1	7.8	1.7	6.1	13.3
CASTEP8	0.5	1.0	1.1	1.1	1.2	4.0	0.7	1.3	1.4	1.6	3.8	1.7	0.8	0.8	1.0	2.1	0.0	2.2	3.2	7.6	2.0	5.6	14.7
CASTEP7	2.4	2.8	3.0	2.9	3.1	5.8	2.6	3.0	2.5	2.8	5.6	3.3	2.6	2.6	2.8	3.5	2.2	0.0	2.3	6.8	3.4	5.7	14.8
CASTEP-MS	3.4	3.7	3.9	3.7	3.9	6.2	3.6	3.8	3.5	3.7	5.6	3.7	3.6	3.5	3.8	4.1	3.2	2.3	0.0	7.6	3.9	6.0	14.3
CASTEP-USP	7.7	7.8	7.9	7.7	7.9	8.9	7.6	7.9	7.9	8.0	8.6	7.4	8.1	7.8	8.0	7.8	7.6	6.8	7.6	0.0	8.2	11.0	13.5
OpenMX	2.0	1.7	1.8	1.8	1.8	3.2	1.9	1.5	2.3	2.5	3.0	1.8	2.2	2.1	2.3	1.7	2.0	3.4	3.9	8.2	0.0	6.4	13.6
DACAPO	6.2	6.5	6.5	6.4	6.4	7.2	6.2	6.5	6.0	6.4	7.6	5.9	6.1	6.3	6.8	6.1	5.6	5.7	6.0	11.0	6.4	0.0	18.4
Abinit_FHI	14.5	13.8	14.0	13.9	14.6	13.6	14.2	13.4	14.2	14.3	13.0	14.1	15.1	14.5	14.5	13.3	14.7	14.8	14.3	13.5	13.6	18.4	0.0

K.Lejaeghere, et al., Science 351, aad3000 (2016)

A data-base of electronic structures

Calculated Electronic Properties of Metals

by

V. L. Moruzzi
J. F. Janak
A. R. Williams

PERGAMON

UPPSALA UNIVERSITET

Electronic structure database

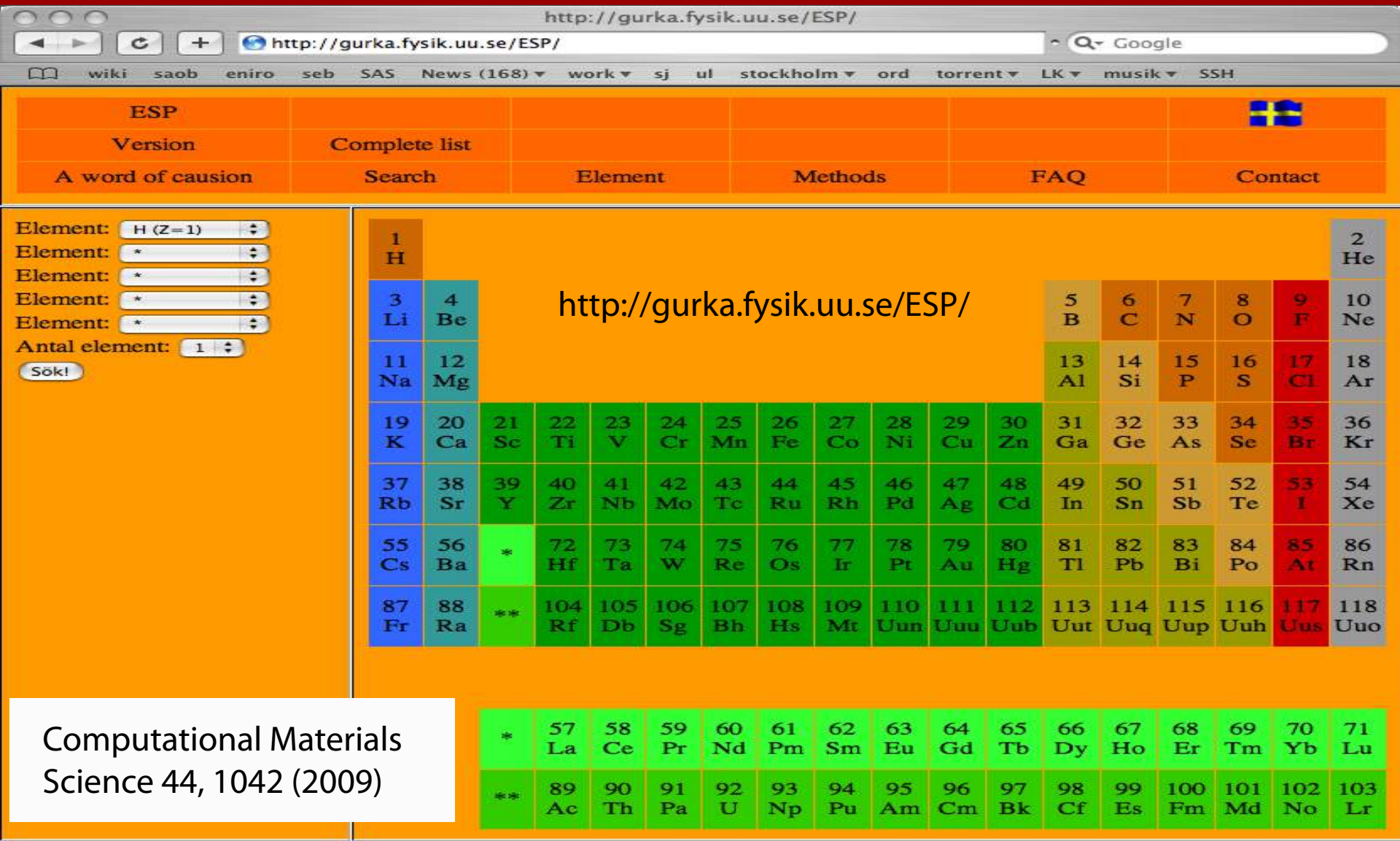

Computational Materials Science 44, 1042 (2009)

Finding new 2D materials

Search criteria

Packing ratio 0.1-0.50
Large gap along one crystallographic direction (>2.5 Å)
No covalent bonds over gap

Results: all known 2D's, including di-chalchogenides
Many new 2D's

New 2D materials (PRX 3, 31002 (2013))

TABLE III. List of compounds found by our algorithm that do not belong to the family of dichalcogenides. The chemical formula, the ICSD number of the corresponding bulk material, the value of the minimum band gap, and an eventual magnetic ordering are given in the different columns from left to right. (The cells of the table are left blank if the material is not magnetically ordered.)

2D chemical formula	3D ICSD number	Gap (eV)	Magnetism	2D chemical formula	3D ICSD number	Gap (eV)	Magnetism
PbIF	150193	2.3		$PbSb_2Te_4$	250250	0.8	
HgI_2	150345	1.8		$KC_6FeO_3N_3$	280850	4.5	
ZrClN	151468	1.9		MgI_2	281551	3.6	
BaIF	155006	4.3		BiIO	391354	1.5	
SrIF	155009	4.5		$FeBr_3$	410924	0.5	AFM
$AlCl_2$	155670	Metal		$MgPSe_3$	413165	2.1	
Ag_2ReCl_6	156662	Metal		IYGa	417149	Metal	
Ni_2Te_2Sb	158485	Metal		PTe_2Ti_2	418978	Metal	
$Bi_{14}Te_{13}S_8$	159356	0.9		ScP_2AgSe_6	420302	1.8	
$MgBr_2$	165972	4.8		$CrSiTe_3$	626809	0.6	FM
Cu_2S	166578	Metal		$FePSe_3$	633094	0.05	
P_2AgSe_6Bi				FeS	633302	Metal	
P_2CuSe_6Bi				FeTe	633877	Metal	FM
YI_3				$Sb_2Ge_2Te_5$	637823	0.2	
GaS				SbSiNi	646436	Metal	
VCl_2	246905	Metal		PbO	647260	2.5	
VBr_2	246906	Metal		CdI_2	655780	2.5	
VI_2	246907	Metal		GaSe	660262	1.8	
PFeLi	247089	Metal		$ZnIn_2S_4$	660273	Metal	
$PbBi_2Te_4$	250249	1.0		$Zn_2In_2S_5$	660333	Metal	

Verified in
Small 11, 1253 (2015)

Are there more high temperature superconductors ?

UPPSALA UNIVERSITET

Data-mining criterion-structure

$Ca_2(CuBr_2O_2)$

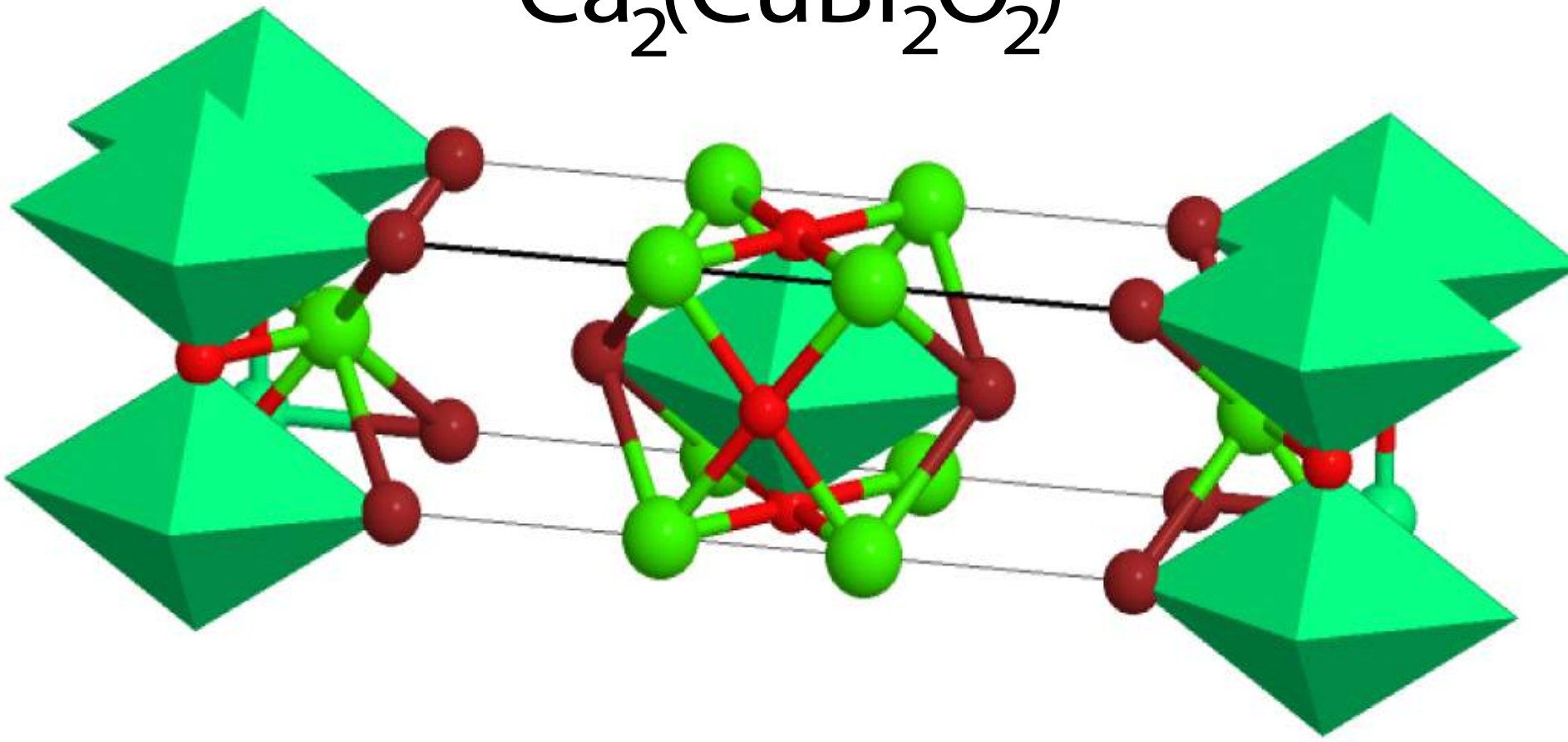

Computational Materials Science 67 282 (2013)

UPPSALA UNIVERSITET

Data-mining criterion-bands/bonds

$Ca_2(CuBr_2O_2)$

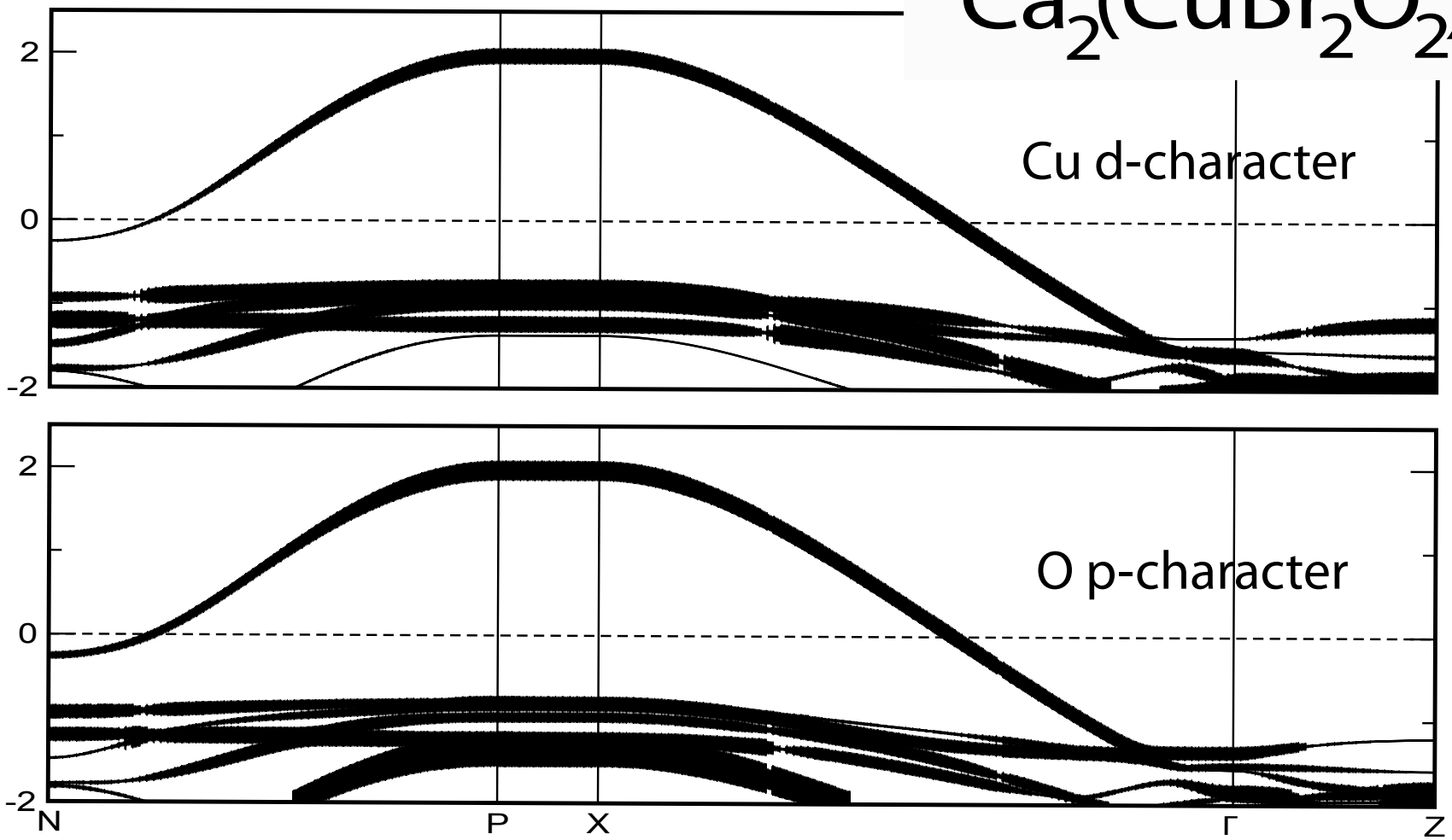

Computational Materials Science 67 282 (2013)

Supplementary information

The table below shows compound name, space group, space group number, bravais lattice and ICSD reference number. Using the ICSD web-site [1], and the ICSD reference number, allows the reader to generate pictures of the crystal structure.

In the fat-band representation the thickness of the band corresponds to the amount of s-, p- or d-character of the band. This is calculated as follows. Let $n(\mathbf{k})$ be the occupation at $\mathbf{k}$ given by

$$n(\mathbf{k}) = Tr(O(\mathbf{k})\rho(\mathbf{k}))$$

where $O(\mathbf{k})$ and $\rho(\mathbf{k})$ is the overlap and density, respectively. The fatness f_l for eigenvalue ν can then be calculated using

$$f_l = \frac{Tr(O(\mathbf{k})\rho^{\nu_l}(\mathbf{k}))}{Tr(O(\mathbf{k})\rho(\mathbf{k}))}$$

where element ij of the density matrix is given in terms of weights (w) and eigenvectors (Z) by:

$$\rho_{ij}(\mathbf{k}) = \sum_{\nu} w_{\nu,\mathbf{k}} Z_i(\mathbf{k},\nu) Z_j^{\dagger}(\mathbf{k},\nu)$$

$$\rho_{ij}^{\nu_l}(\mathbf{k}) = w_{\nu_l,\mathbf{k}} Z_i(\mathbf{k},\nu_l) Z_j^{\dagger}(\mathbf{k},\nu_l)$$

$\sum_l f_l$ sums up to one electron and l runs over the complete basis. Note that in the figures below the Fermi level is at zero. Also, in the band plots we make a projection on atomic and l-resolved fat bands.

[1] G. Bergerhoff and I. D.Brown, in Crystallographic Databases, F. H. Allen et al. (Hrsg.) Chester, International Union of Crystallography, (1987). The figures were generated using ICSD Web (http:icsd.fiz-karlsruhe.de/icsd) using version 2.1.0.

Material	Space group	(#)	Bravais lattice	ICSD #
$AuCuZn_2$	F m -3 m	(225)	cubic face-centred	150571
$AgAuZn_2$	F m -3 m	(225)	cubic face-centred	604792
$CuNi_2Sb$	F m -3 m	(225)	cubic face-centred	53320
$CuNi_2Sn$	F m -3 m	(225)	cubic face-centred	103068
$ErPt_2$	F d -3 m S	(227)	cubic face-centred	103287
$EuPt_2$	F d -3 m S	(227)	cubic face-centred	103430
$HoPt_2$	F d -3 m S	(227)	cubic face-centred	104441
$NaPt_2$	F d -3 m S	(227)	cubic face-centred	644945
$BaPt_2$	F d -3 m S	(227)	cubic face-centred	616039
CuSe	P 63/m m c	(194)	hexagonal primitive	240
KAuTe	P 63/m m c	(194)	hexagonal primitive	40165
RbAuTe	P 63/m m c	(194)	hexagonal primitive	75026
$CdInGaS_4$	P -3 m 1	(164)	hexagonal primitive	20785
ZrNCl	P -3 m 1	(164)	hexagonal primitive	25506
KCuSe	P 63/m m c	(194)	hexagonal primitive	12157
KCuTe	P 63/m m c	(194)	hexagonal primitive	12158
Li_2ZnGe	P -3 m 1	(164)	hexagonal primitive	53678
Li_2ZnSi	P -3 m 1	(164)	hexagonal primitive	16221
$AuYO_2$	P 63/m m c	(194)	hexagonal primitive	95675
$AgAlO_2$	P 63/m m c	(194)	hexagonal primitive	300020
CuBr	P 63 m c	(186)	hexagonal primitive	30092
$Ca_2CuZn_2P_3$	P 63/m m c	(194)	hexagonal primitive	89517
Al_5C_3N	P 63 m c	(186)	hexagonal primitive	26859
$Ca_3Cu_2Zn_2P_4$	P -3 m 1	(164)	hexagonal primitive	89515
$Eu_3Cu_2Zn_2P_4$	P -3 m 1	(164)	hexagonal primitive	89516
$Cu_4(S_2)_2(CuS)_2$	P 63/m m c	(194)	hexagonal primitive	26968

Material	Space group	(#)	Bravais lattice	ICSD #
$LaKPdO_3$	C 1 2/m 1	(12)	monoclinic base-centred	417108
BaY_2F_8	C 1 2/m 1	(12)	monoclinic base-centred	74359
AgCuS	C m c m	(63)	orthorhombic base-centred	30233
$LaSeTe_2$	C m c m	(63)	orthorhombic base-centred	413171
NbS_2	C m 2 m	(38)	orthorhombic base-centred	67443
$BaNiY_2O_5$	I m m m	(71)	orthorhombic body-centred	68795
$RuOCl_2$	I m m m	(71)	orthorhombic body-centred	83883
$Bi_2(CO_3)O_2$	I m m 2	(44)	orthorhombic body-centred	94740
$Al_2Ba_3Ge_2$	I m m m	(71)	orthorhombic body-centred	52612
$Ba_3Al_2Si_2$	I m m m	(71)	orthorhombic body-centred	100128
$Ba_3Al_2Sn_2$	I m m m	(71)	orthorhombic body-centred	9565
$NbSe_2$	F m 2 m	(42)	orthorhombic face-centred	71339
TaS_2	F m 2 m	(42)	orthorhombic face-centred	280988
TaS_2	F 2 m m	(42)	orthorhombic face-centred	67651
$TaSe_2$	F m 2 m	(42)	orthorhombic face-centred	72198
$Tl_2Ba_2CuO_6$	F m m m	(69)	orthorhombic face-centred	41569
TiNCl	P m m n S	(59)	orthorhombic primitive	27396
$Pb_2Ba_2YCuCu_2O_8$	P 2 21 2	(17)	orthorhombic primitive	66088
$Pb_2Sr_2YCu_3O_8$	P 2 21 2	(17)	orthorhombic primitive	66587
$YBa_2Cu_3O_{6.5}$	P m m m	(47)	orthorhombic primitive	75697
$YBa_2Cu_3O_{6.5}$	P m m m	(47)	orthorhombic primitive	96016
$EuBa_2Cu_3O_7$	P m m m	(47)	orthorhombic primitive	81171
$Ba_2GdCu_3O_7$	P m m m	(47)	orthorhombic primitive	56514
$HoBa_2Cu_3O_7$	P m m m	(47)	orthorhombic primitive	68044
$LaBa_2Cu_3O_7$	P m m m	(47)	orthorhombic primitive	81167
$NdBa_2Cu_3O_7$	P m m m	(47)	orthorhombic primitive	81169
$PrBa_2Cu_3O_7$	P m m m	(47)	orthorhombic primitive	81168
$SmBa_2Cu_3O_7$	P m m m	(47)	orthorhombic primitive	71705
$Ba_2YCu_3O_7$	P m m m	(47)	orthorhombic primitive	202770
$Ba_2YCu_3O_7$	P m m m	(47)	orthorhombic primitive	77737
$LaBa_2Cu_3O_8$	P m m m	(47)	orthorhombic primitive	85291
$Na_3Cu_4S_4$	P b a m	(55)	orthorhombic primitive	10004
$Sr_4V_3O_{10}$	I 4/m m m	(139)	tetragonal body-centred	73698
MoB	I 41/a m d S	(141)	tetragonal body-centred	24280
WB	I 41/a m d S	(141)	tetragonal body-centred	24281
$Yb(AgS_2)$	I 41 m d	(109)	tetragonal body-centred	27091
LaI_2	I 4/m m m	(139)	tetragonal body-centred	202452
$SmCu_2Si_2$	I 4/m m m	(139)	tetragonal body-centred	106843
$TbCu_2Si_2$	I 4/m m m	(139)	tetragonal body-centred	106844
Cu_2TmSi_2	I 4/m m m	(139)	tetragonal body-centred	53349
Cu_2YSi_2	I 4/m m m	(139)	tetragonal body-centred	23551
Li_2PdH_2	I 4/m m m	(139)	tetragonal body-centred	108534
Na_2PdH_2	I 4/m m m	(139)	tetragonal body-centred	68071
$(Cu_2S_2)(Sr_2NiO_2)$	I 4/m m m	(139)	tetragonal body-centred	88424
$Ca_2(CuBr_2O_2)$	I 4/m m m	(139)	tetragonal body-centred	1028
$Sr_2CoO_2Br_2$	I 4/m m m	(139)	tetragonal body-centred	151789
$CuSr_2Br_2O_2$	I 4/m m m	(139)	tetragonal body-centred	1178
$Ca_2(CuCl_2O_2)$	I 4/m m m	(139)	tetragonal body-centred	1027
$Ca_2CuO_2Cl_2$	I 4/m m m	(139)	tetragonal body-centred	83117
$Sr_2CuO_2Cl_2$	I 4/m m m	(139)	tetragonal body-centred	4087
$Tl_2Ba_2CaCu_2O_8$	I 4/m m m	(139)	tetragonal body-centred	78592
$Bi_2Sr_2CaCu_2O_8$	I 4/m m m	(139)	tetragonal body-centred	68188
Ce_2BiO_2	I 4/m m m	(139)	tetragonal body-centred	9099
Ce_2SbO_2	I 4/m m m	(139)	tetragonal body-centred	9100
$CePd_2Si_2$	I 4/m m m	(139)	tetragonal body-centred	621852
$CePt_2Si_2$	I 4/m m m	(139)	tetragonal body-centred	52895
Cu_2ErGe_2	I 4/m m m	(139)	tetragonal body-centred	53251
$ErCu_2Si_2$	I 4/m m m	(139)	tetragonal body-centred	106845
Cu_2GdSi_2	I 4/m m m	(139)	tetragonal body-centred	64825

Material	Space group	(#)	Bravais lattice	ICSD #
Cu_2HoGe_2	I 4/m m m	(139)	tetragonal body-centred	53270
YCu_2Ge_2	I 4/m m m	(139)	tetragonal body-centred	52764
Cu_2HoSi_2	I 4/m m m	(139)	tetragonal body-centred	53289
$NdCu_2Si_2$	I 4/m m m	(139)	tetragonal body-centred	106842
$Eu_2(VO_4)$	I 4/m m m	(139)	tetragonal body-centred	89000
$K_2(NiF_4)$	I 4/m m m	(139)	tetragonal body-centred	15576
$K_2(NiF_4)$	I 4/m m m	(139)	tetragonal body-centred	631720
$Rb_2(NiF_4)$	I 4/m m m	(139)	tetragonal body-centred	69682
$La_2(NiO_4)$	I 4/m m m	(139)	tetragonal body-centred	1179
$La_2(NiO_4)$	I 4/m m m	(139)	tetragonal body-centred	33536
La_2PdO_4	I 4/m m m	(139)	tetragonal body-centred	40262
$Sr_2(MoO_4)$	I 4/m m m	(139)	tetragonal body-centred	152123
$Sr_2(RuO_4)$	I 4/m m m	(139)	tetragonal body-centred	157401
Sr_2VO_4	I 4/m m m	(139)	tetragonal body-centred	72219
Cs_2AgF_4	I 4/m m m	(139)	tetragonal body-centred	16254
K_2CoF_4	I 4/m m m	(139)	tetragonal body-centred	33522
Rb_2CoF_4	I 4/m m m	(139)	tetragonal body-centred	69683
$Gd_2(CuO_4)$	I 4/m m m	(139)	tetragonal body-centred	41844
In_2CuO_4	I 4/m m m	(139)	tetragonal body-centred	39475
$La_2(CuO_4)$	I 4/m m m	(139)	tetragonal body-centred	41643
Ba_2CoF_6	I 4/m m m	(139)	tetragonal body-centred	21057
Ba_2NiF_6	I 4/m m m	(139)	tetragonal body-centred	21056
$Ba_2(ZnF_6)$	I 4/m m m	(139)	tetragonal body-centred	21054
$(Cu_2S_2)(Sr_2CuO_2)$	I 4/m m m	(139)	tetragonal body-centred	88423
$Ba_2Cu_3O_4Br_2$	I 4/m m m	(139)	tetragonal body-centred	36128
$Ba_2Cu_3O_4Cl_2$	I 4/m m m	(139)	tetragonal body-centred	355
$Ca_3Cu_2O_4Br_2$	I 4/m m m	(139)	tetragonal body-centred	69182
$Ca_3Cu_2O_4Cl_2$	I 4/m m m	(139)	tetragonal body-centred	69181
$La_3Ni_2O_6$	I 4/m m m	(139)	tetragonal body-centred	249209
$K_3Ni_2F_7$	I 4/m m m	(139)	tetragonal body-centred	33523
$Sr_3V_2O_7$	I 4/m m m	(139)	tetragonal body-centred	71320
$Sr_3(V_2O_7)$	I 4/m m m	(139)	tetragonal body-centred	71451
$K_3Co_2F_7$	I 4/m m m	(139)	tetragonal body-centred	33524
$K_3Cu_2F_7$	I 4/m m m	(139)	tetragonal body-centred	15373
$La_4Ni_3O_8$	I 4/m m m	(139)	tetragonal body-centred	173372
K_5Te_3	I 4/m	(87)	tetragonal body-centred	96743
$CaSmCuO_3Cl$	P 4/n m m Z	(129)	tetragonal primitive	86428
$HgBa_2CaCu_2O_6$	P 4/m m m	(123)	tetragonal primitive	75725
$HgBa_2CaCu_2O_6$	P 4/m m m	(123)	tetragonal primitive	83087
$TlYBa_2Cu_2O_7$	P 4/m m m	(123)	tetragonal primitive	74163
$TlCaSr_2Cu_2O_7$	P 4/m m m	(123)	tetragonal primitive	74165
$NdBa_2Cu_2NbO_8$	P 4/m m m	(123)	tetragonal primitive	44255
Sr_2CoO_3Cl	P 4/n m m Z	(129)	tetragonal primitive	91750
$HgBa_2CuO_4$	P 4/m m m	(123)	tetragonal primitive	75720
$Sr_2CuO_2(CO_3)$	P 4 21 2	(90)	tetragonal primitive	83096
$KCeSe_4$	P 4/n b m Z	(125)	tetragonal primitive	67656
$NdLi_2Sb_2$	P 4/n m m Z	(129)	tetragonal primitive	36020
$HgBa_2Ca_2Cu_3O_8$	P 4/m m m	(123)	tetragonal primitive	75730
$HoBa_2Cu_3O_6$	P 4/m m m	(123)	tetragonal primitive	68047
$LuBa_2Cu_3O_6$	P 4/m m m	(123)	tetragonal primitive	98113
$NdBa_2Cu_3O_6$	P 4/m m m	(123)	tetragonal primitive	83074
$Cs(Cu_4Se_3)$	P 4/m m m	(123)	tetragonal primitive	75196
KCu_4S_3	P 4/m m m	(123)	tetragonal primitive	23336
KCu_4Se_3	P 4/m m m	(123)	tetragonal primitive	280072

A data-base for Ce compounds

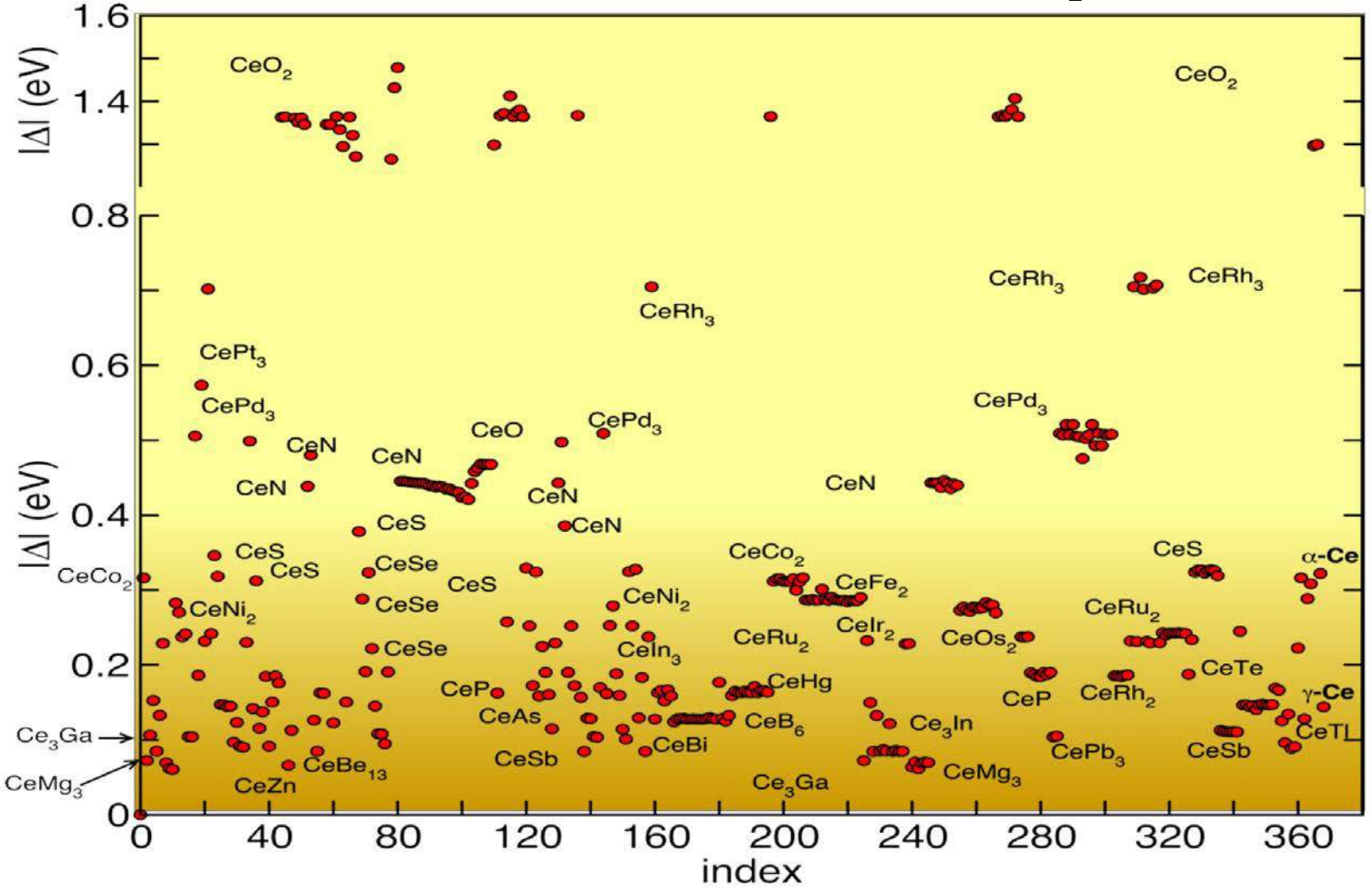

$$\Delta(E)=(E-H)-G_0^{-1}$$

Kondo temperatures

$$T_{\mathrm{K}} = \alpha \exp\left[-\frac{2}{(2J+1)J_{\mathrm{K}}\,\rho(E_{\mathrm{F}})}\right] \qquad J_{\mathrm{K}} = \frac{2\Delta^2(E_{\mathrm{F}})}{(E_f - E_{\mathrm{F}})}$$

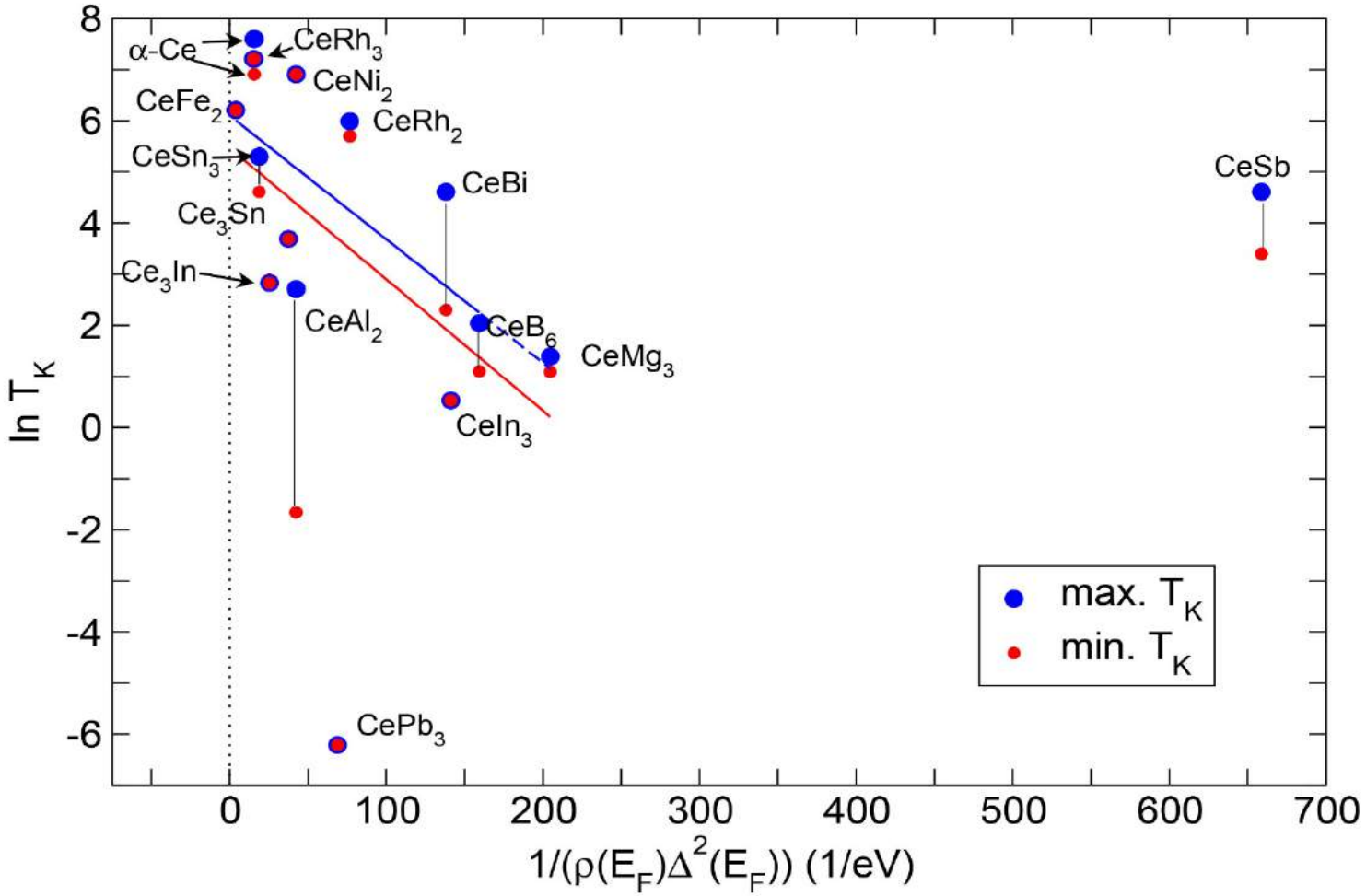

Some experience with DMFT

UPPSALA UNIVERSITET

Spectra (XPS)

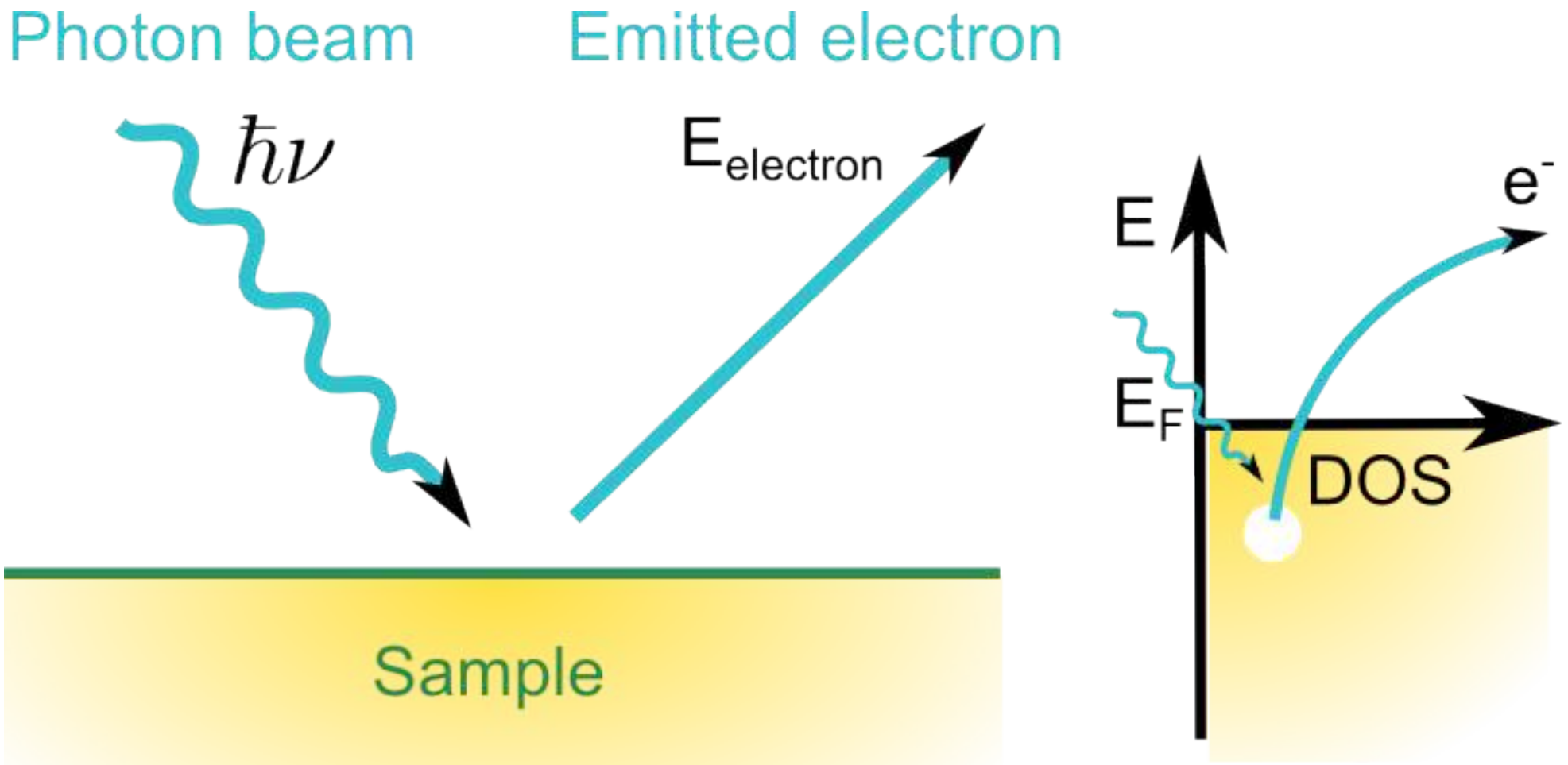

UPPSALA UNIVERSITET

NiO - an example

ÖREBRO UNIVERSITET

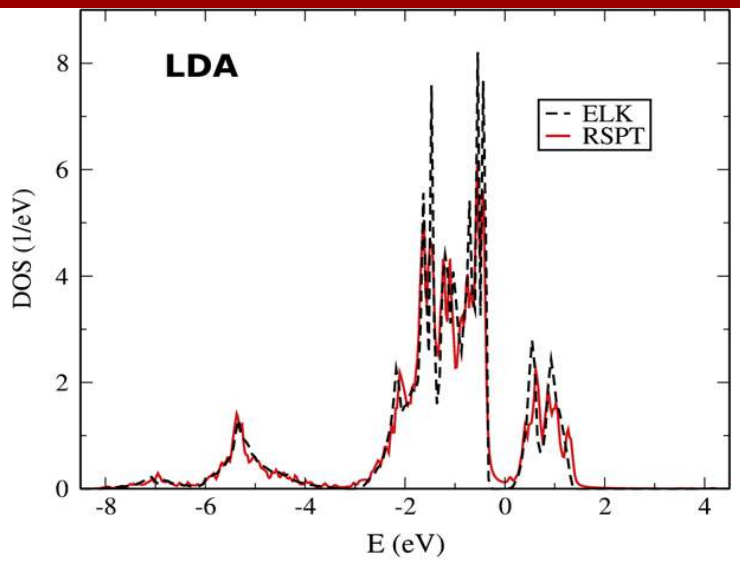

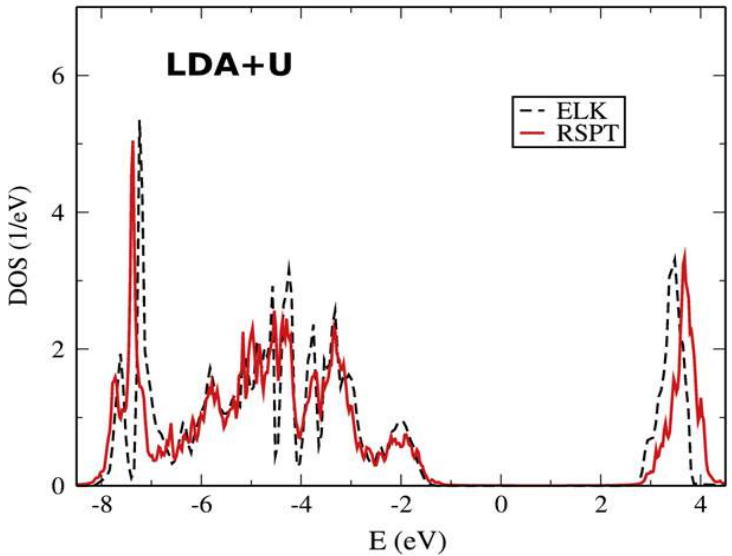

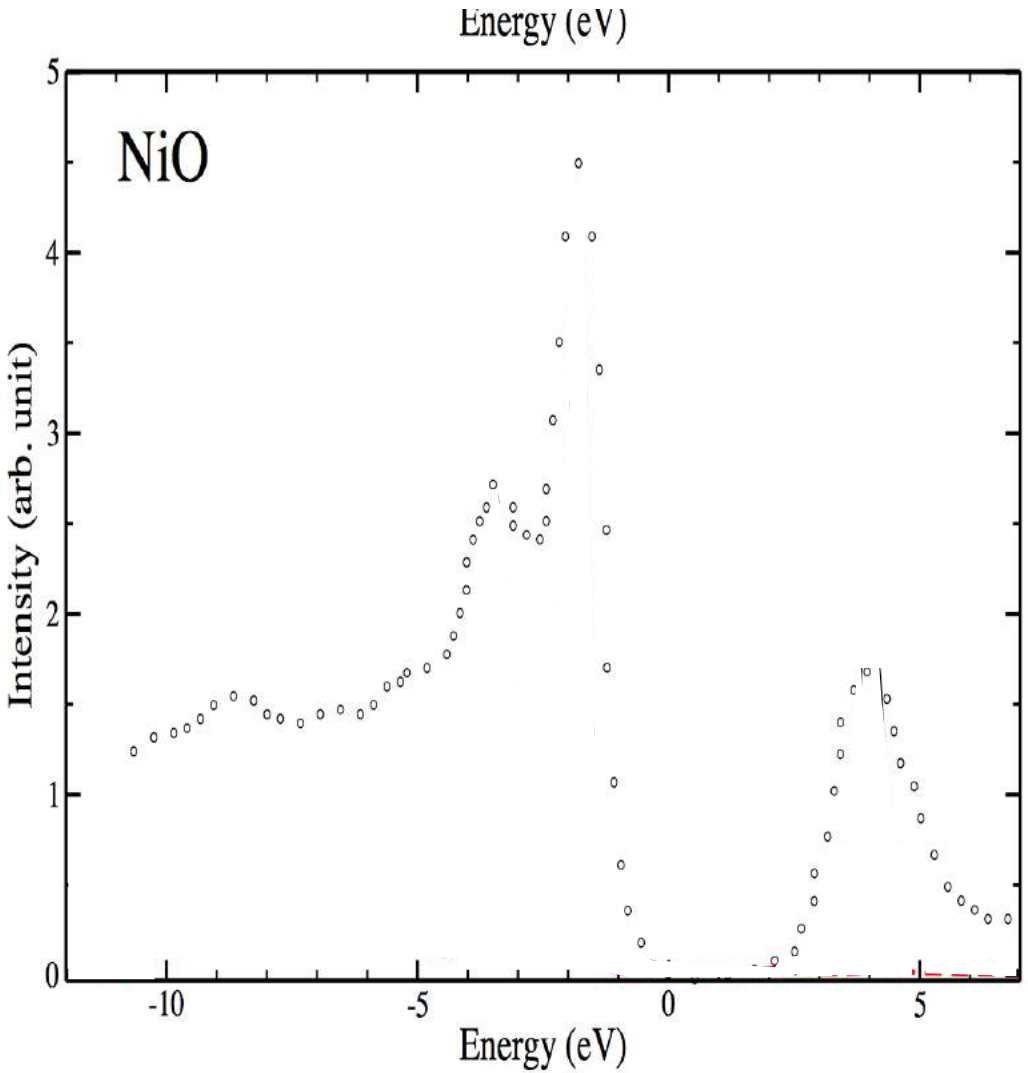

UPPSALA UNIVERSITET

Correlated basis

$$\hat{\boldsymbol{A}}_R \equiv \sum_{\xi,\xi'} |R,\xi\rangle\langle R,\xi| \sum_{\mathbf{k}} \hat{\boldsymbol{A}}_{\mathbf{k}} |R,\xi'\rangle\langle R,\xi'|$$

Two choices of $|R,\xi\rangle$, muffin-tin based and orthogonal:

i) MT

$$|\xi >= i^l Y_{lm}\phi_l$$

ii) ORT

$$(\mathbf{H} - \epsilon\mathbf{O})\mathbf{x} = 0$$

$$\mathbf{O} = \mathbf{L}\mathbf{L}^h$$

Cholesky decomposition gives

$$(\mathbf{L}^{-1}\mathbf{H}\mathbf{L}^{-h} - \epsilon\mathbf{1})\mathbf{y} = 0$$

$$\mathbf{y} = \mathbf{L}^h\mathbf{x}$$

Dynamical mean field theory

UPPSALA UNIVERSITET

$$H = H_{LDA} + \sum_{R} \sum_{\xi_1\xi_2\xi_3\xi_4} U_{\xi_1\xi_2\xi_3\xi_4} c^{\dagger}_{R\xi_1} c^{\dagger}_{R\xi_2} c_{R\xi_3} c_{R\xi_4}$$

U-matrix expressed in terms of Slater integrals

The Hubbard model is mapped into an Anderson Impurity Model

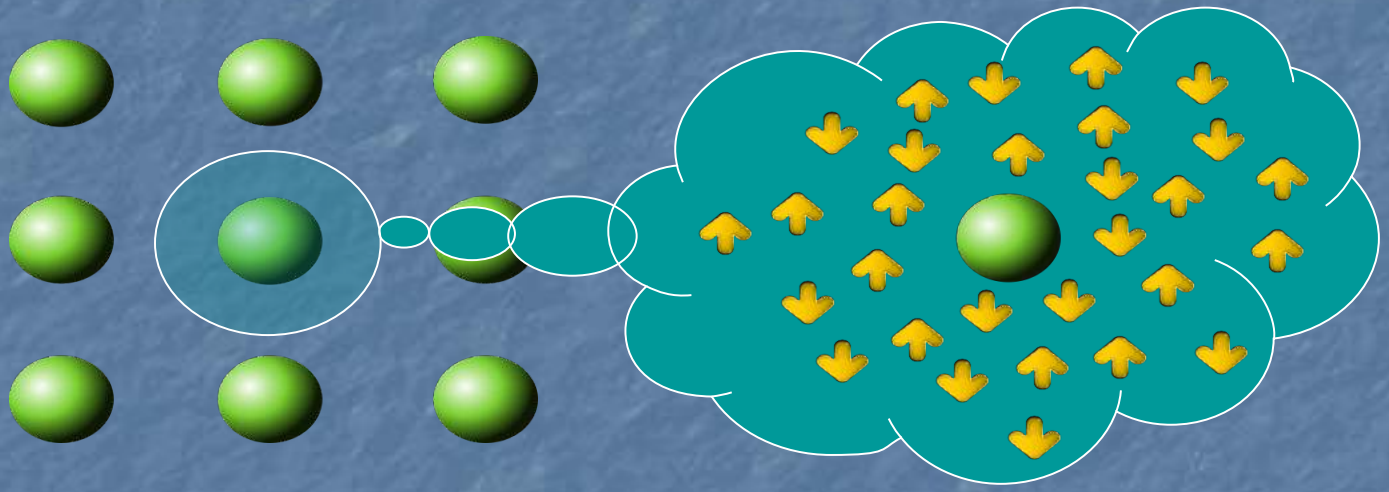

FICTITIOUS SYSTEM REPRODUCING THE DYNAMICS

The mapping is made with the condition of preserving the local Green's function and is exact in the limit of infinite nearest neighbors

Exact Diagonalization Solver

The finite size problem can be solved exactly with a direct construction of all the accessible many-body states.

N=5 electrons in K=10 orbitals:

$$
\begin{aligned}
|\Psi_1^5\rangle &= |1111100000\rangle, \\
|\Psi_2^5\rangle &= |1111010000\rangle, \\
&\vdots \\
|\Psi_M^5\rangle &= |0000011111\rangle.
\end{aligned}
$$

M corresponds to $\binom{K}{N}$

Too large for standard computational resources!

Block diagonalization ⟶ up to 30 bath states!

Exact Diagonalization Solver

The finite size problem can be solved exactly with a direct construction of all the accessible many-body states.

N=5 electrons in K=10 orbitals:

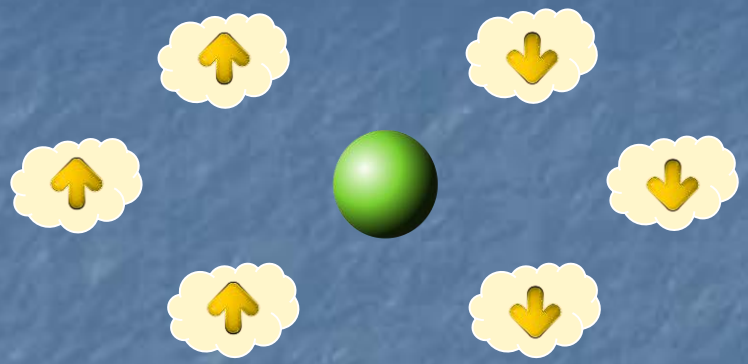

Once the many-body states have been determined, the one-particle Green's function can be obtained through the Lehmann representation

$$G^{\mathrm{ED}}(i\omega)_{\xi_1\xi_2} = \frac{1}{Z}\sum_{\nu\mu}\frac{\langle\mu|\hat{c}_{\xi_1}|\nu\rangle\langle\nu|\hat{c}^{\dagger}_{\xi_1}|\mu\rangle}{i\omega + E_\mu - E_\nu}\left(e^{-\beta E_\mu} + e^{-\beta E_\nu}\right)$$

Paramagnetic NiO

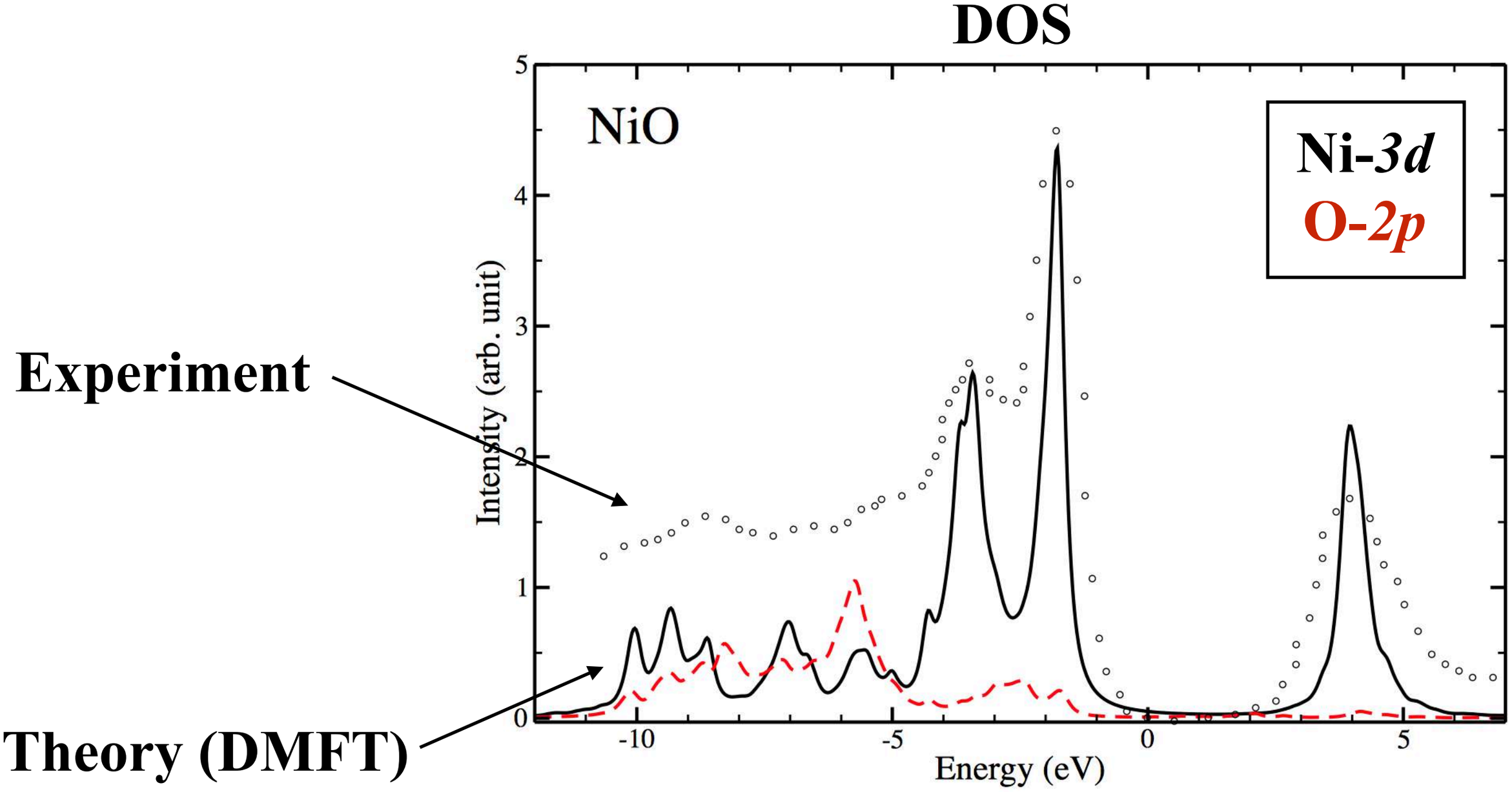

P. Thunström *et al.* PRL **109** 186401 (2012)

UPPSALA UNIVERSITET

Valence band of Mn-doped GaAs

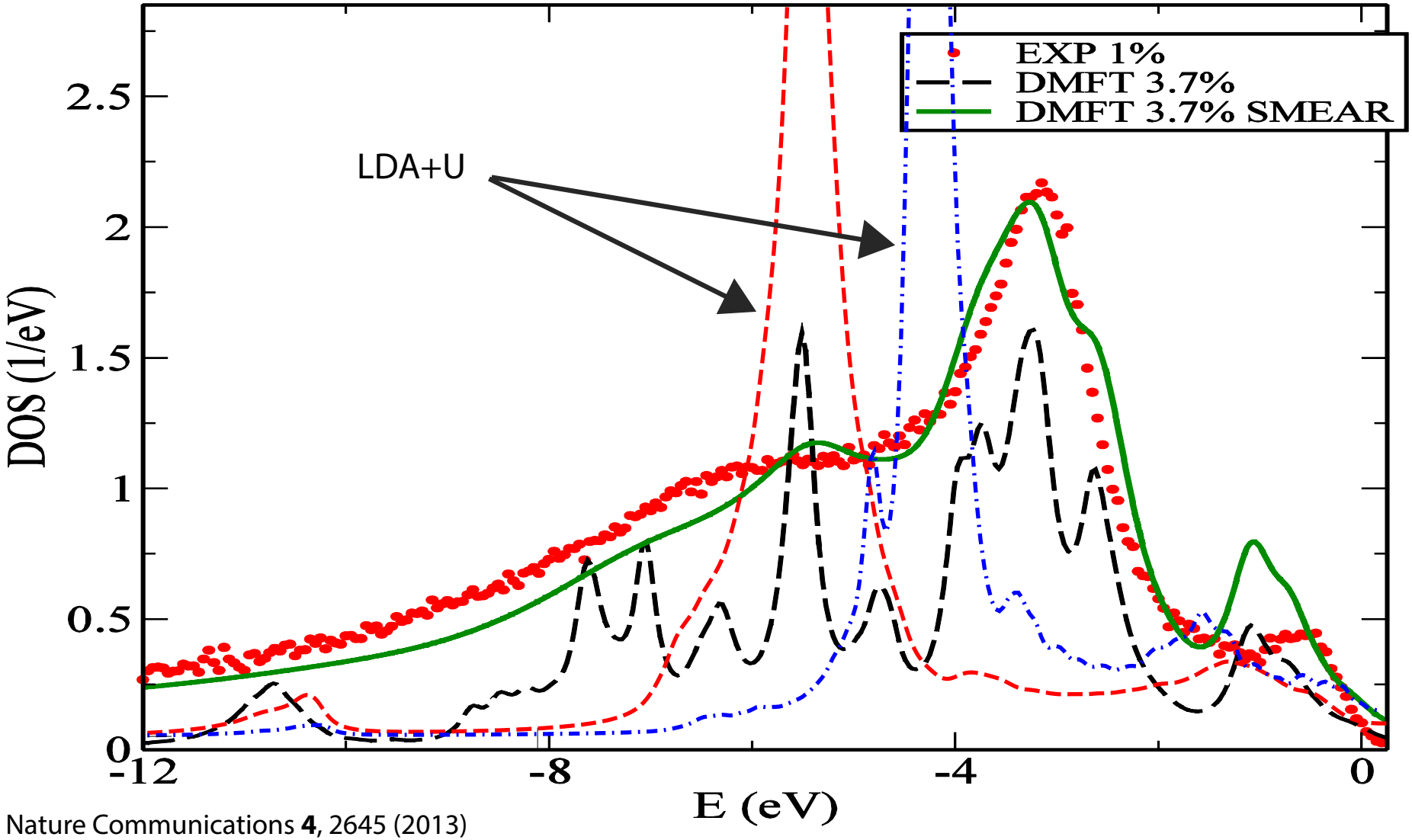

Nature Communications **4**, 2645 (2013)

UPPSALA UNIVERSITET

Valence band spetra of rare-earths

(Loch et al. PRB 2016)

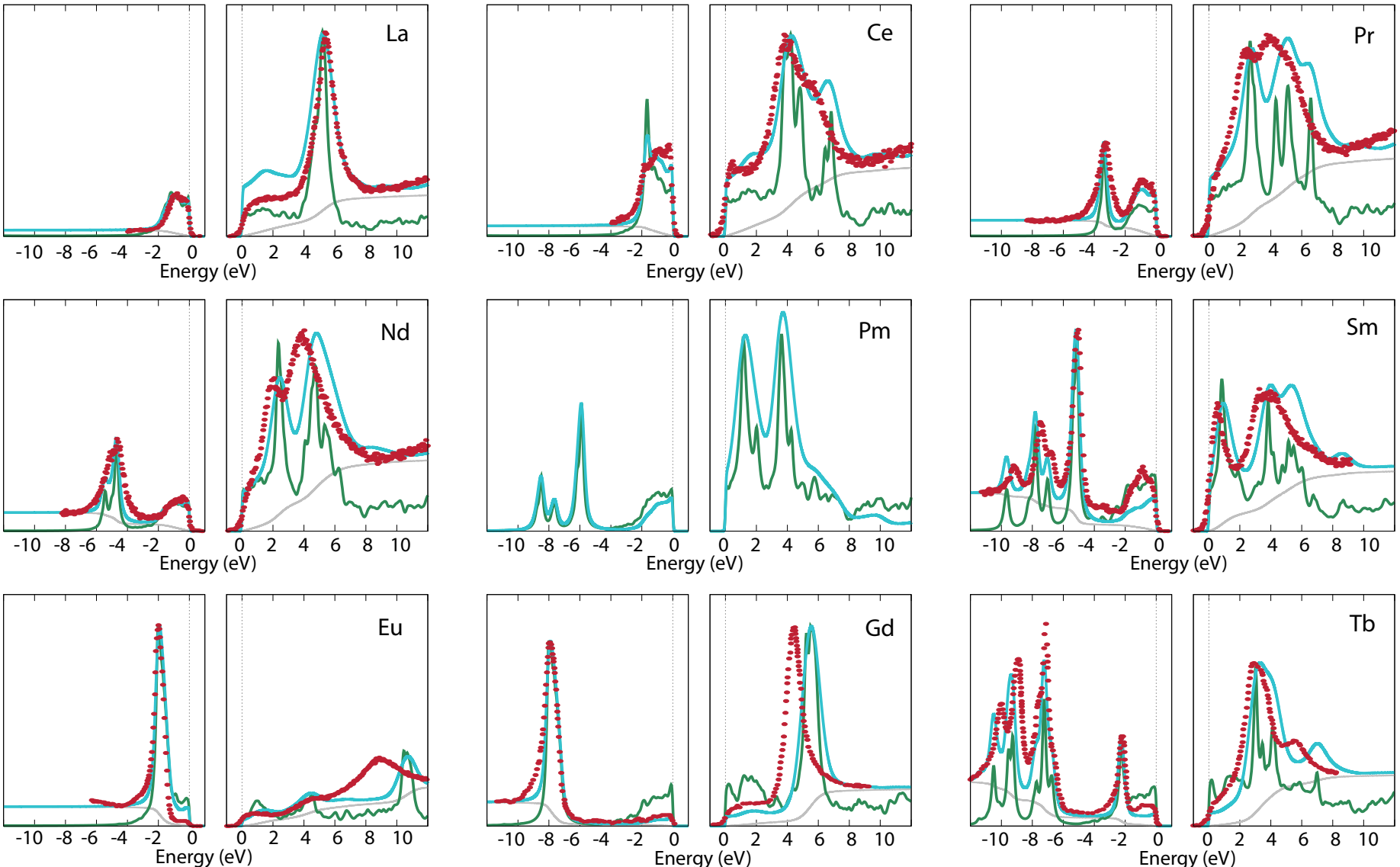

UPPSALA UNIVERSITET

Valence band spetra of rare-earths

(Loch et al. PRB 2016)

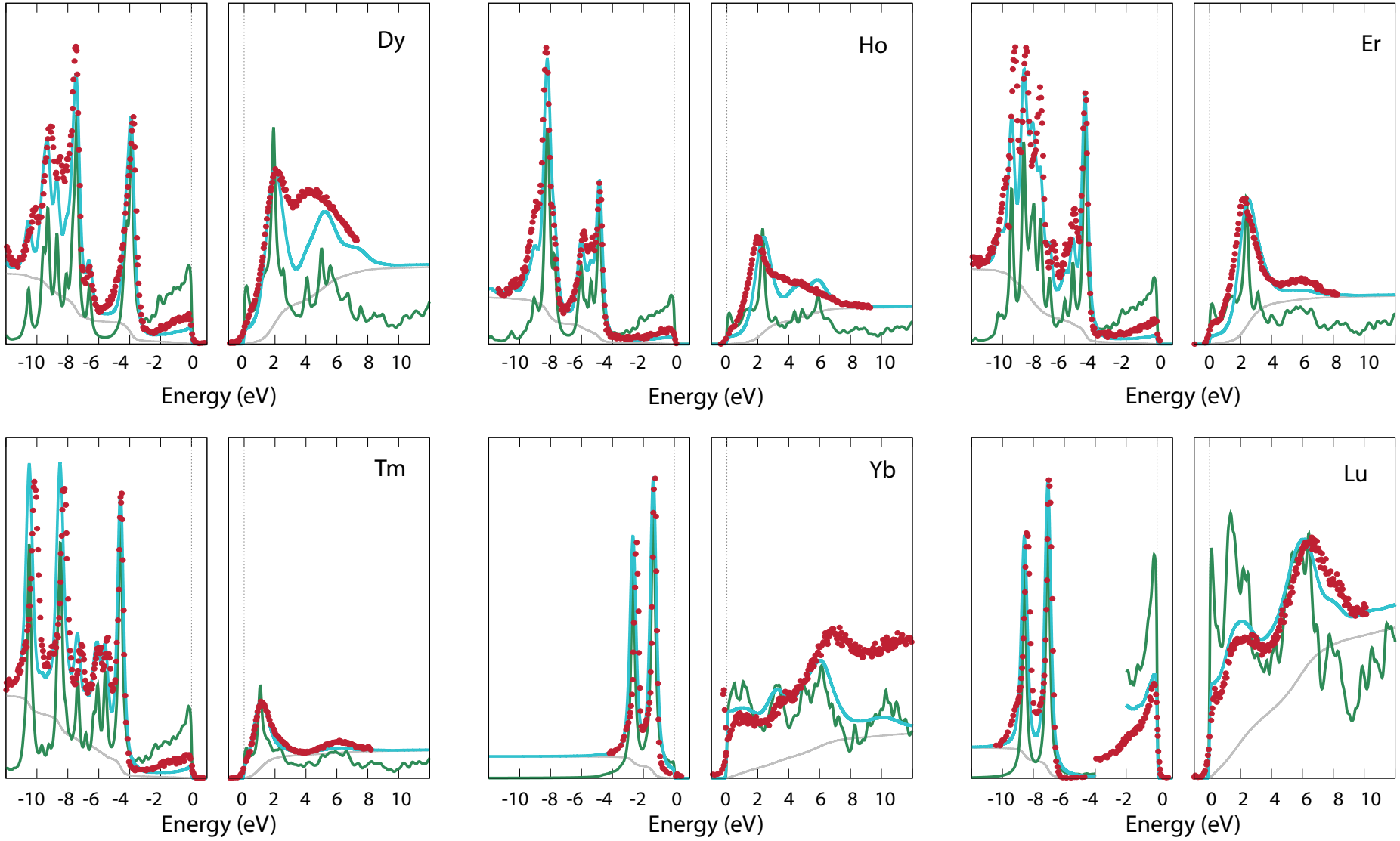

The XAS process

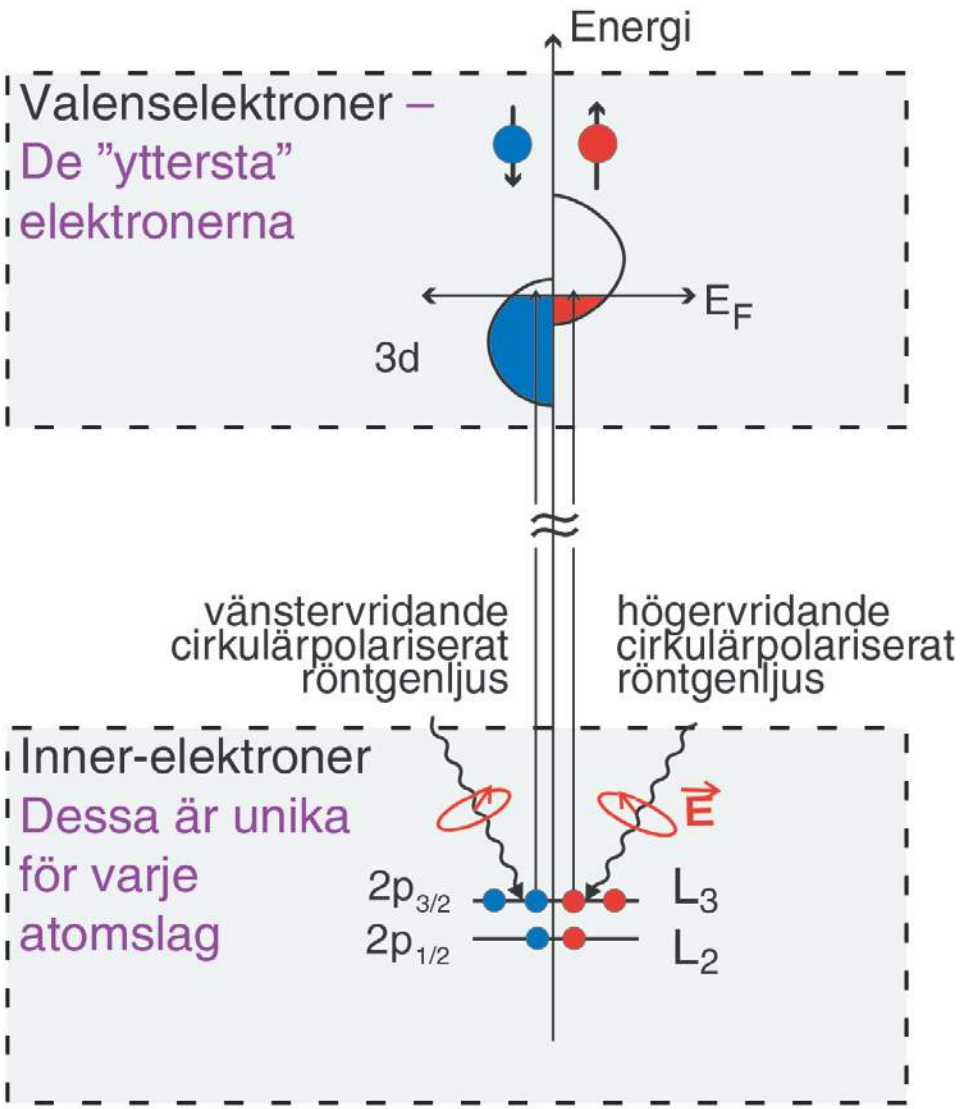

UPPSALA UNIVERSITET

Hamiltonians

The initial state SIAM Hamiltonian:

$$\hat{H}_{init} = \sum_{ij} \varepsilon_{3d,ij} \hat{d}_i^+ \hat{d}_j + \sum_{ij} \varepsilon_{L,ij} \hat{L}_i^+ \hat{L}_j + \sum_{ij} V_{ij}^{3dL} \left[\hat{d}_i^+ \hat{L}_j + \hat{L}_j^+ \hat{d}_i \right] + \lambda_{3d} \sum_{n} \hat{\vec{l}}_{3d,n}^{+} \cdot \hat{\vec{s}}_{3d,n} + \sum_{ijkl} U_{ijkl}^{3d3d} \hat{d}_i^+ \hat{d}_j^+ \hat{d}_l \hat{d}_k$$

$\sum_{ij} \varepsilon_{3d,ij} \hat{d}_i^+ \hat{d}_j$ splitting of the 3d levels (10Dq)

$\sum_{ij} \varepsilon_{L,ij} \hat{L}_i^+ \hat{L}_j$ and of the ligand states following the symmetry of the 3d

$\sum_{ij} V_{ij}^{3dL} \left[\hat{d}_i^+ \hat{L}_j + \hat{L}_j^+ \hat{d}_i \right]$ coupling between ligands and *d* orbitals

[1] P.W. Andersson, Phys. Rev. 124, 41 (1961).

UPPSALA UNIVERSITET

Final state

The final state XAS Hamiltonian accounts in addition for the 2p to 3d excitations (Quanty):

$$\hat{H}_{XAS} = \hat{H}_{init} + \sum_{ij} \varepsilon_{2p} \hat{p}_i^{+} \hat{p}_j + \lambda_{2p} \sum_{n} \hat{\vec{l}}_{2p,n}^{+} \cdot \hat{\vec{s}}_{2p,n} + \sum_{ijkl} U_{ijkl}^{2p3d} \hat{d}_i^{+} \hat{p}_j^{+} \hat{p}_l \hat{d}_k$$

Computed L-edge X-Ray Absorption Spectra

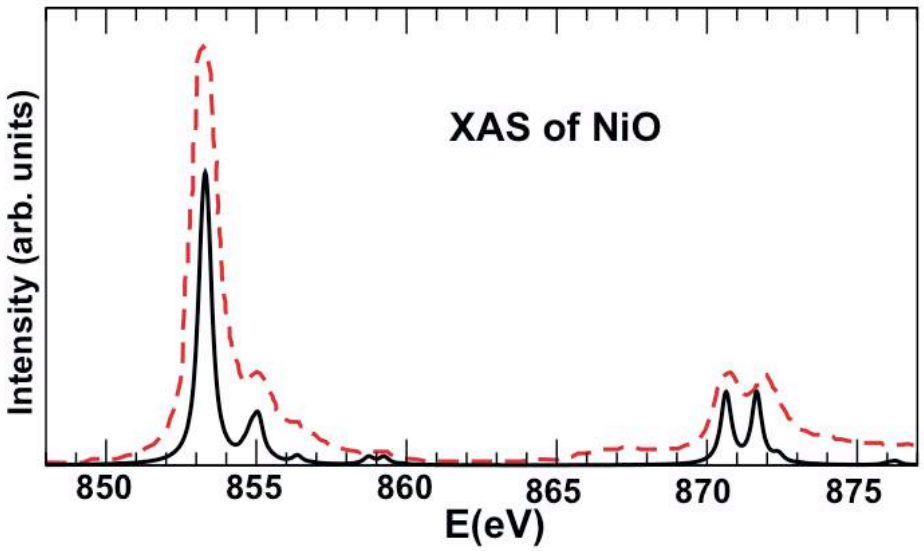

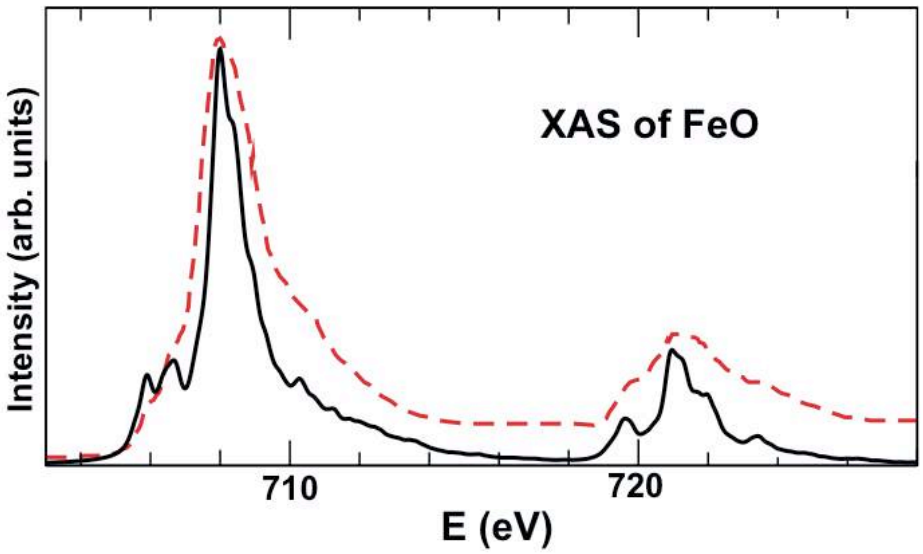

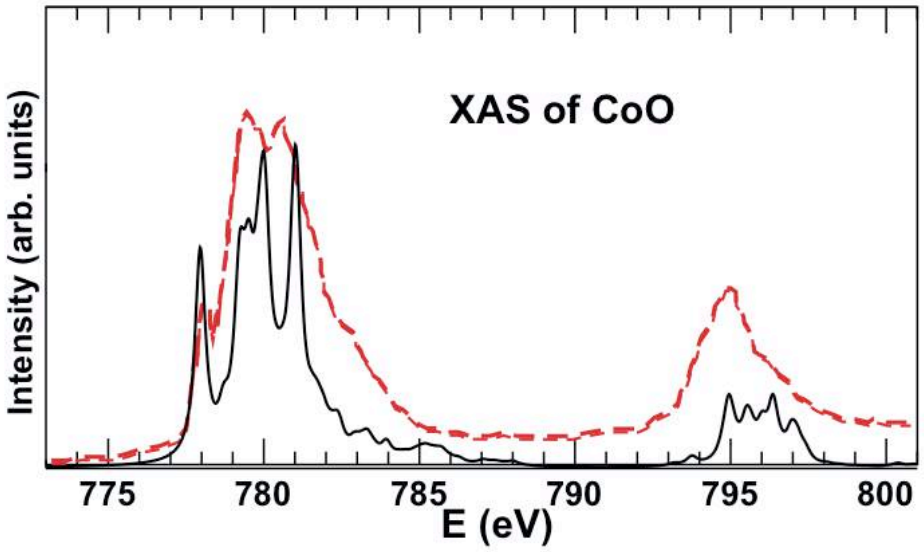

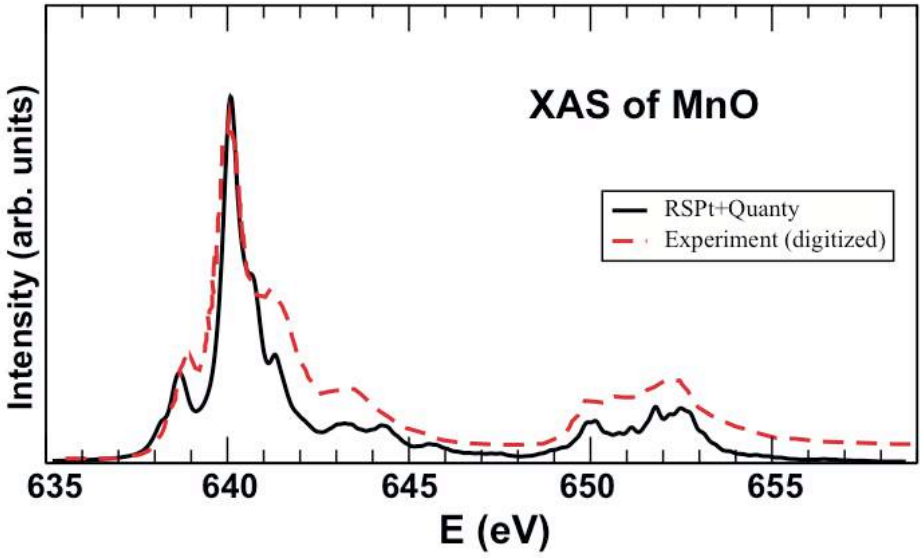

Experimental scenario: STM image

Constant-current topograph (10 mV, 0.5 nA)

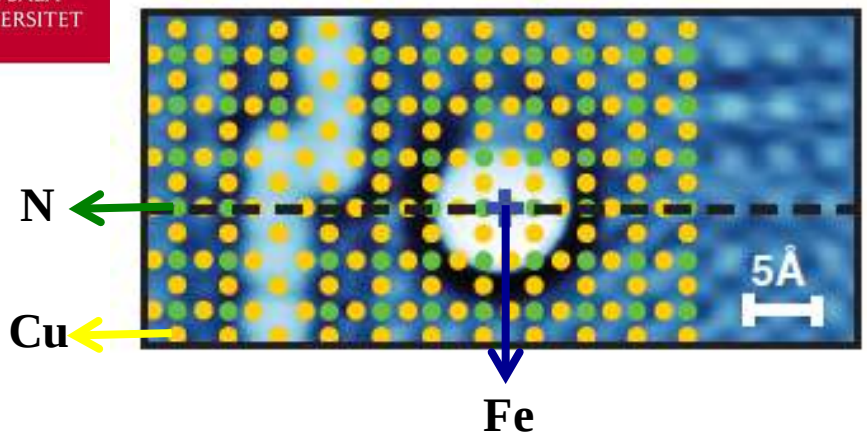

Cross section of the unfiltered topograph

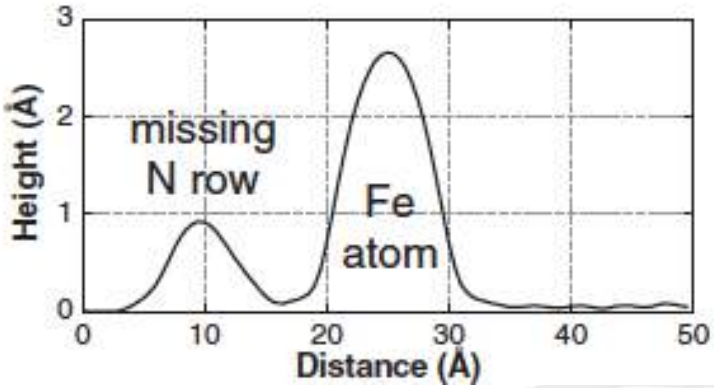

- **Experimental system:** a single atomic layer of CuN to decouple the spin of the Fe atom from the underlying Cu (100) surface.

- **Cross section-** Fe atom has large apparent height of 2.6 Å.

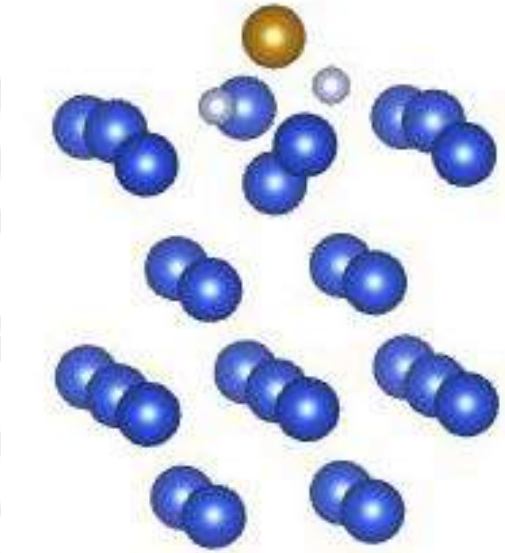

Science **317**, 1199 (2007)

Conduction spectra

B || N (z-axes) B || Hollow (x-axes) B || out-of-plane (y-axes)

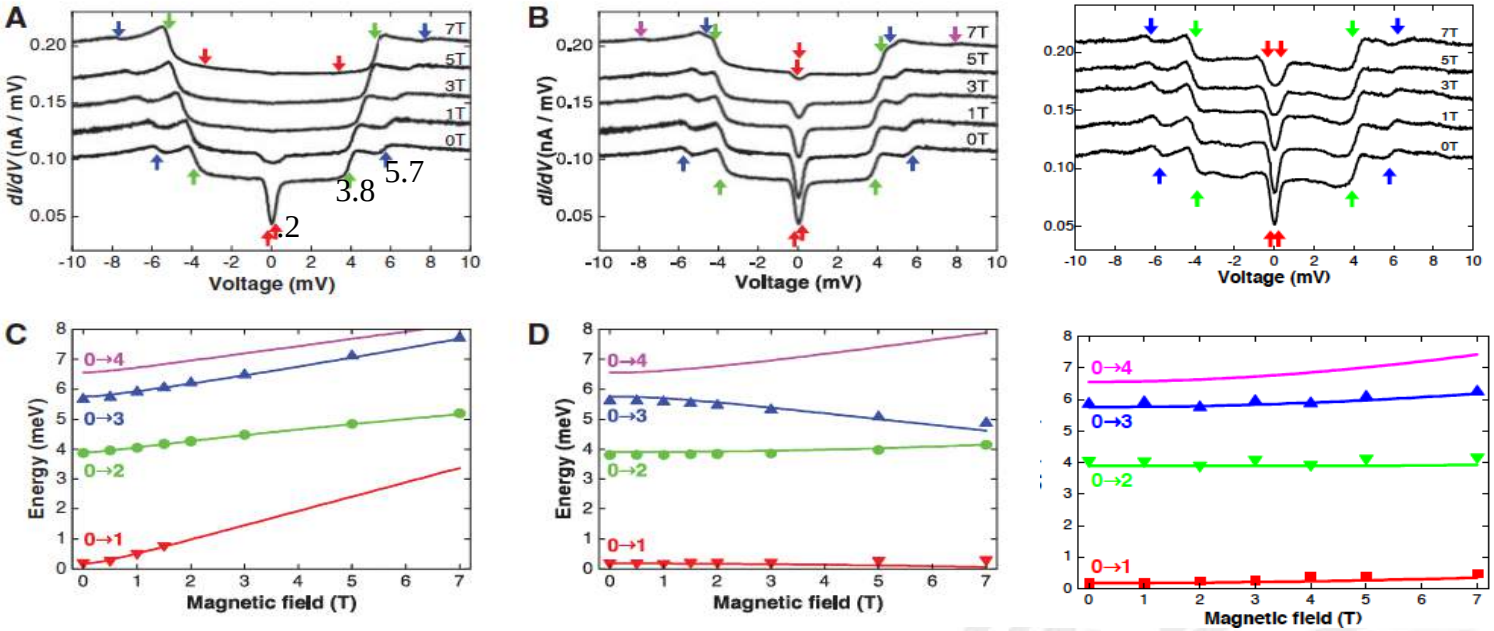

- The changes in the excitation energies are markedly different when the magnetic field is applied in the three different directions- **evidence of strong magnetic anisotropy**.
- **Spin Hamiltonian:** $H = g\mu_B \mathbf{B}.\mathbf{S} + D S_z^2 + E(S_x^2 - S_y^2)$

  Zeeman **Axial** **Transverse magnetic anisotropy**
- **Using the spin of a free Fe atom (S = 2), a best fit of all of the excitations give g = 2.11, D = –1.55 meV, and E = 0.31 meV.**
- **Primary anisotropy axis:** along the N direction-**indication of the importance of local molecular bonding for magneto crystalline anisotropy.**

Science **317**, 1199 (2007)

Spin excitation spectra for B=0

Spin Hamiltonian $H = D S_z^2 + E(S_x^2 - S_y^2) = D S_z^2 + E/2(S_+^2 + S_-^2)$

When S = 2, m_s = -2, -1 , 0, +1, +2

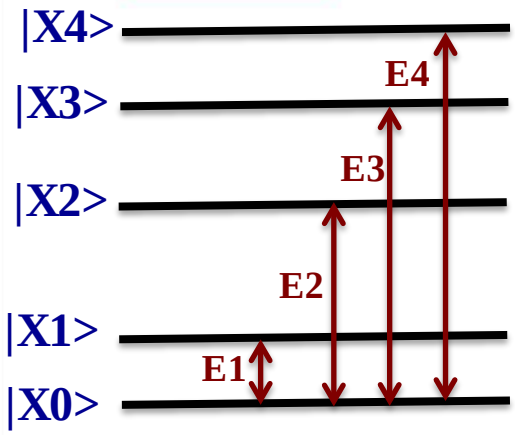

For experimental D = -1.55, E = 0.31

The eigen states are

|X0> = -0.6973 |2> + 0.1660 |0> - 0.6973 |-2>

|X1> = -0.7071 |2> - 0.7071|-2>

|X2> = 0.7071 |1> - 0.7071 |-1>

|X3> = 0.7071 |1> + 0.7071 |-1>

|X4> = -0.1174 |2> -0.9860 |0> - 0.1174 |-2>

$$\begin{pmatrix} 4D & 0 & \sqrt{6}E & 0 & 0 \\ 0 & D & 0 & 3E & 0 \\ \sqrt{6}E & 0 & 0 & 0 & \sqrt{6}E \\ 0 & 3E & 0 & D & 0 \\ 0 & 0 & \sqrt{6}E & 0 & 4D \end{pmatrix}$$

	E1	E2	E3	E4
Exp	**0.18**	**3.90**	**5.76**	**6.56**
LSDA	0.09	0.99	1.71	1.87
LSDA+U	0.10	1.06	1.84	2.00
HIA (FLL)	0.36	1.46	1.70	2.41
ED	0.49	5.32	6.34	7.68

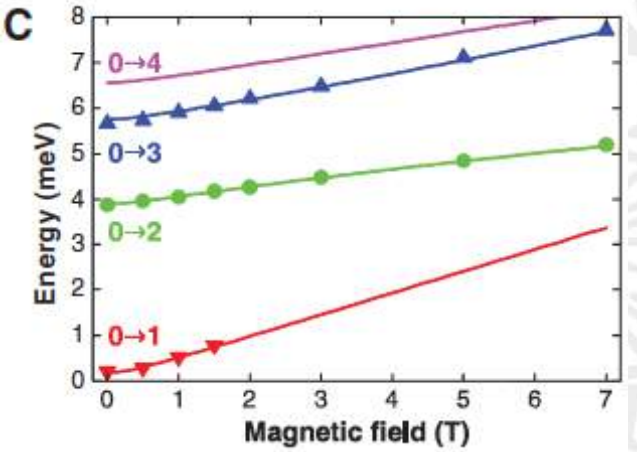

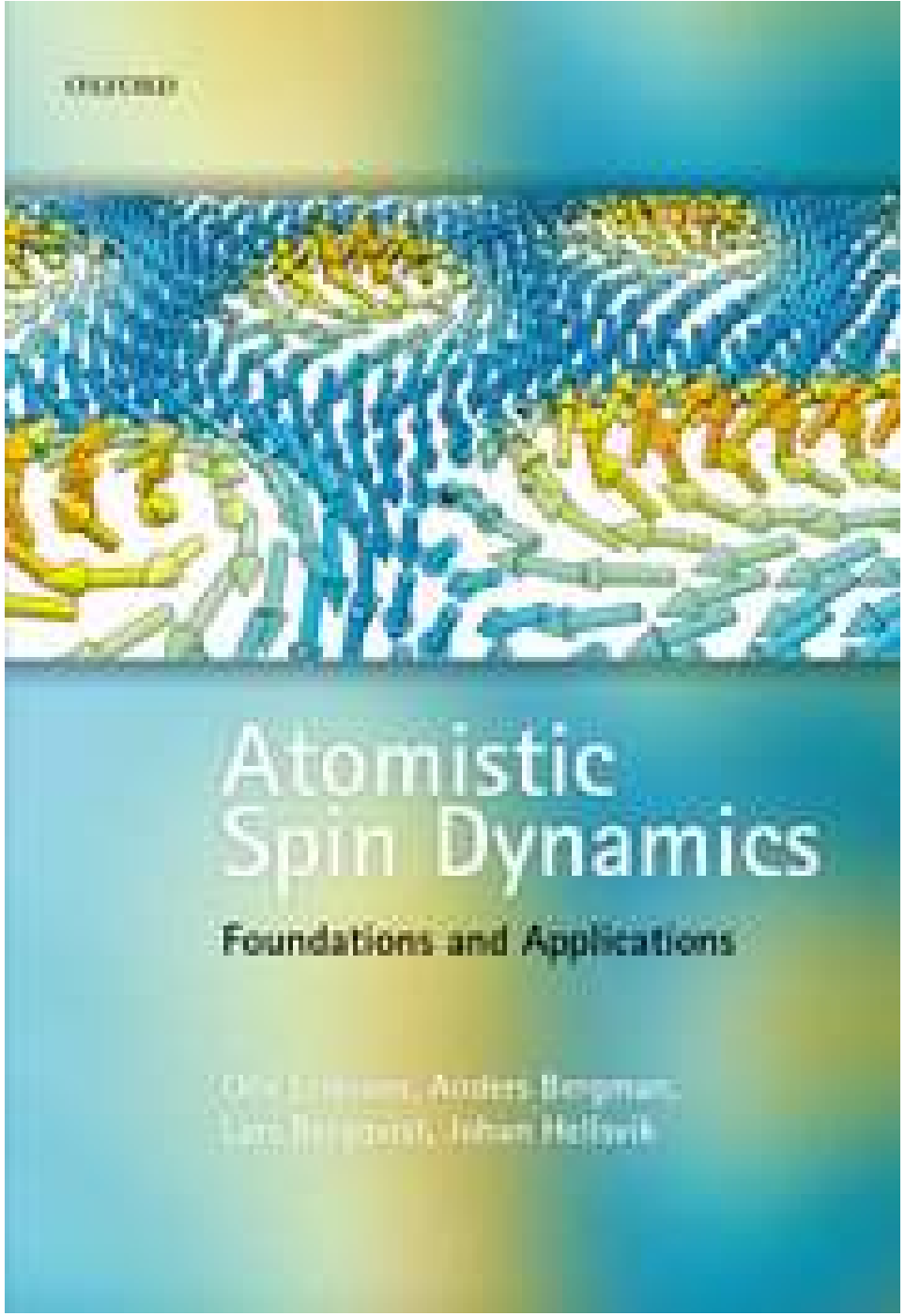
OXFORD
Atomistic
Spin Dynamics
Foundations and Applications

Magnetic properties

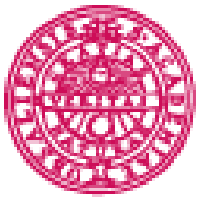

UPPSALA
UNIVERSITET

Magnetism i historien

ÖREBRO UNIVERSITET

UPPSALA UNIVERSITY

Galileos compass

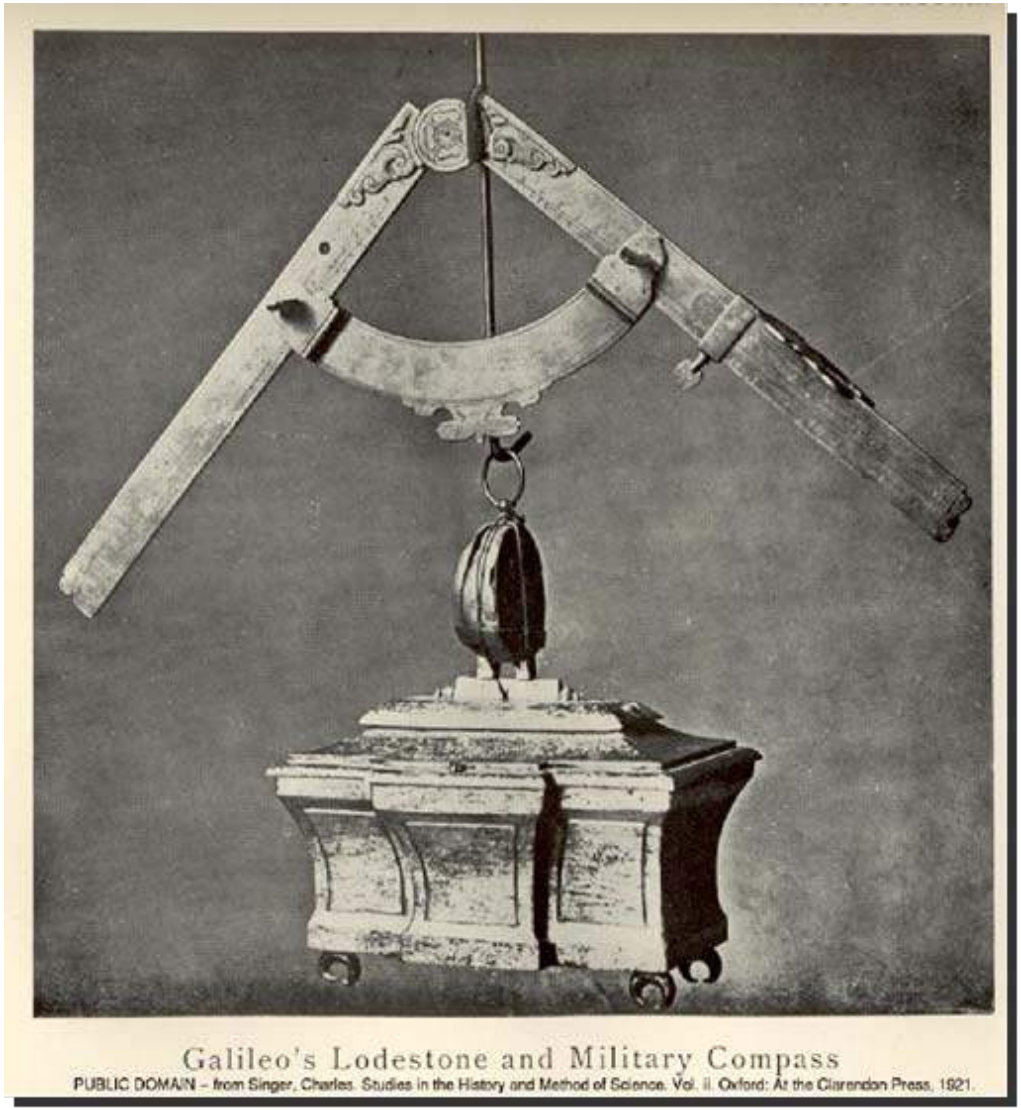

Galileo's Lodestone and Military Compass

PUBLIC DOMAIN – from Singer, Charles. Studies in the History and Method of Science. Vol. ii. Oxford: At the Clarendon Press, 1921.

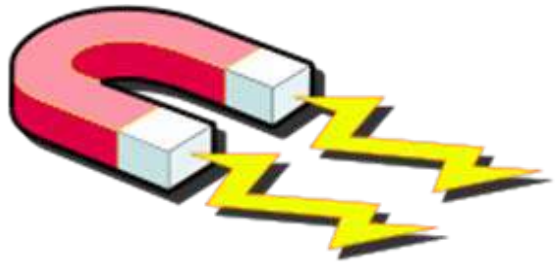

- Magnetic Interaction lead to mechanical forces and torque

UPPSALA UNIVERSITET

Spin moments of Fe-Co alloys

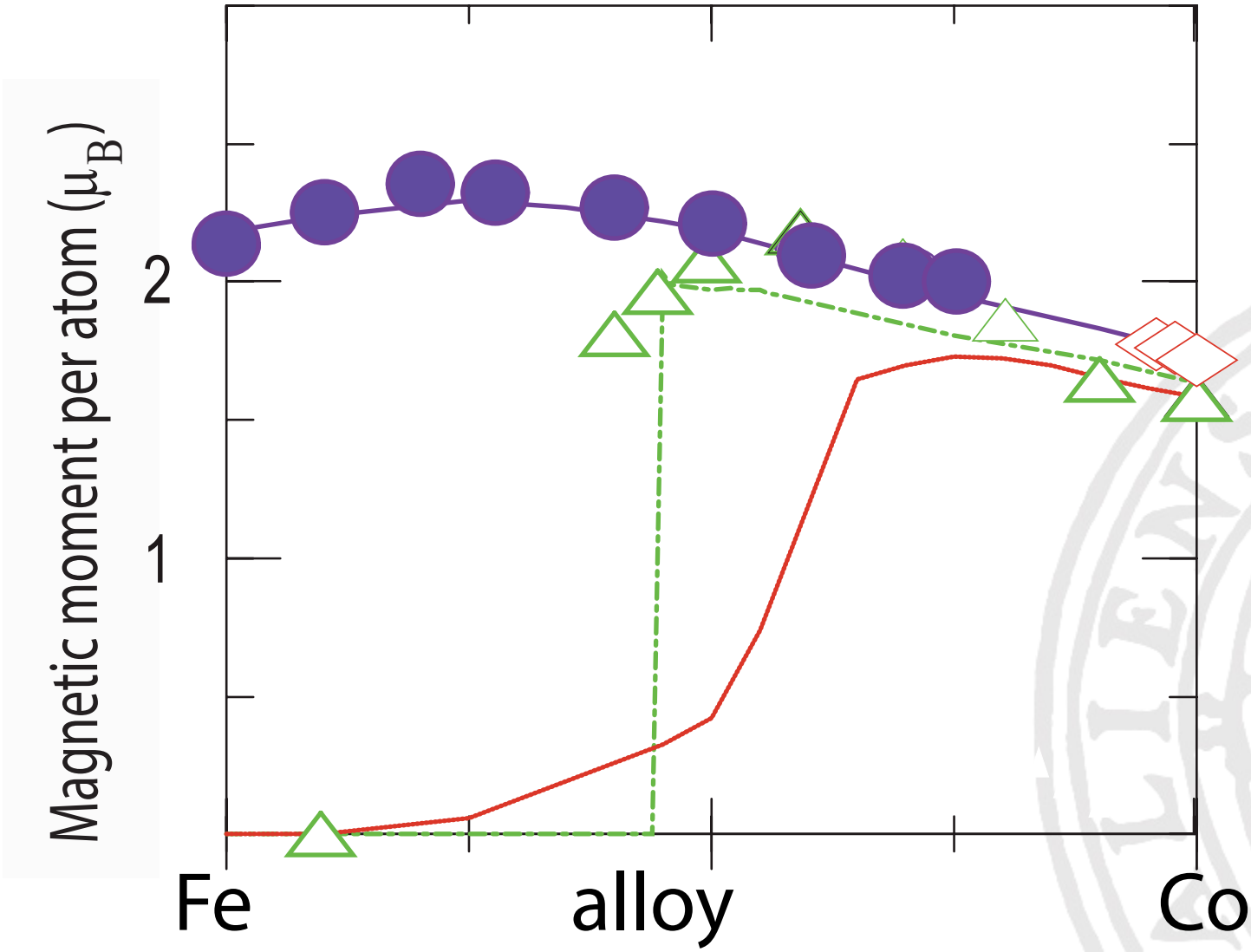

PHYSICAL REVIEW B 59, 419 (1999)

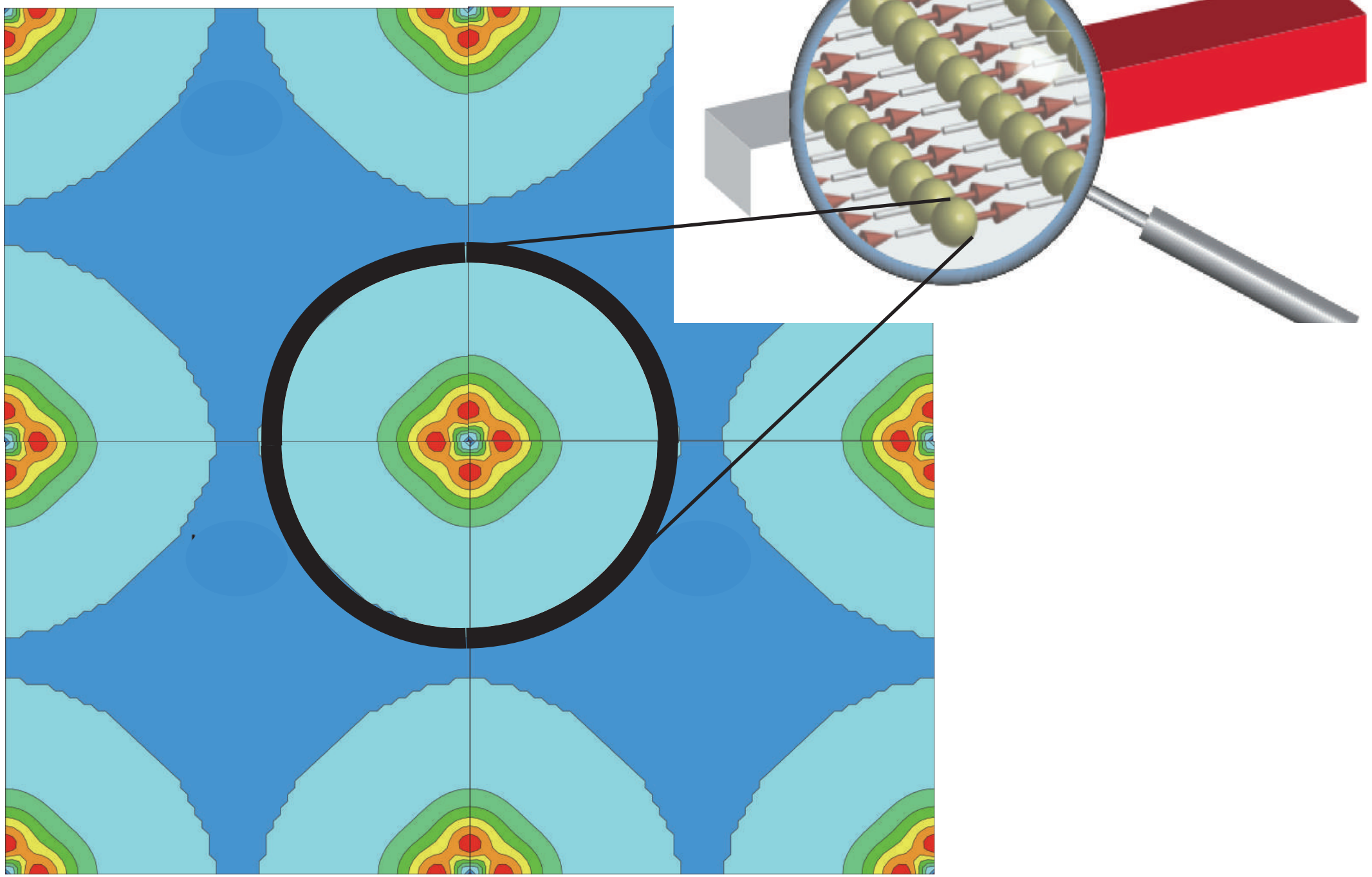

UPPSALA UNIVERSITET

Heisenberg Model

- A picture of localised spins
- Magnetization is a “classical” vector, assigned to each site

$$\hat{H} = -\sum_{i \neq j} J_{ij} \cdot (\vec{e}_i \cdot \vec{e}_j)$$

With $\vec{e}_i = \dfrac{\vec{S}_i}{|\vec{S}_i|}$

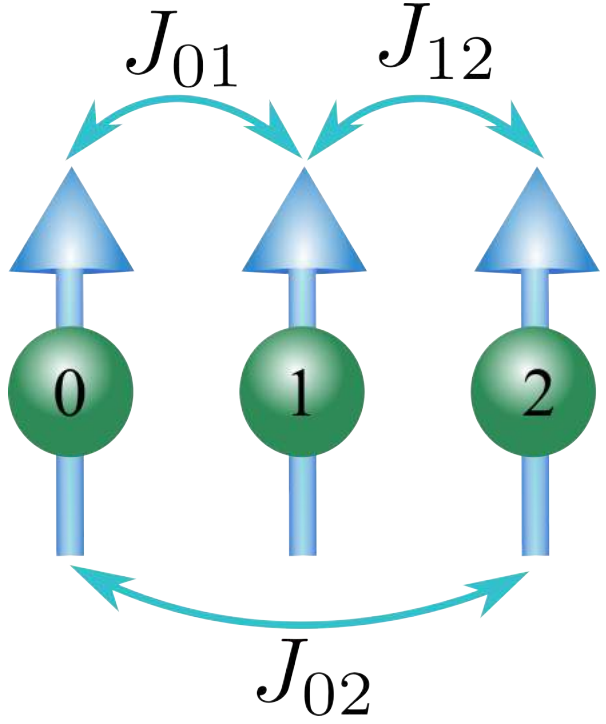

UPPSALA UNIVERSITET

Exchange parameters

Expansion of the Hamiltonian in $\delta\vec{\theta}_i$ and $\delta\vec{\theta}_j$ gives

$$J_{ij} = \frac{-1}{4\pi}\int_{-\infty}^{E_F} \delta\epsilon \mathrm{Tr}_m \left[\Delta_i \cdot G_{ij}^{\uparrow}(\epsilon) \cdot \Delta_j \cdot G_{ij}^{\downarrow}(\epsilon)\right]$$

Local exchange field

$$\Delta_i = (\hat{H}_i^{\uparrow} - \hat{H}_i^{\downarrow})$$

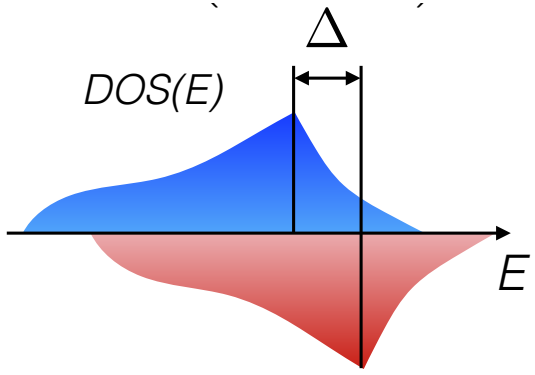

Inter-site Greens function

$$G_{ij}^{\sigma} = \left\langle i \left| \hat{G}(z) \right| j \right\rangle = \left\langle i \left| \frac{1}{z - \hat{H}^{\sigma}} \right| j \right\rangle$$

Lichtenstein *et al* JMMM **67** 65 (1987),
Katsnelson *et al* PRB **61** 8906 (2000),
Kvashnin *et al* PRB **91** 125133 (2015)

UPPSALA UNIVERSITET

Heisenberg spin Hamiltonian

$$H_{spin} = -\sum_{<ij>} J_{ij}\mathbf{S}_i \cdot \mathbf{S}_j \qquad H_{spin} = -J\sum_{<ij>} \mathbf{S}_i \cdot \mathbf{S}_j$$

M vs T for bcc Fe

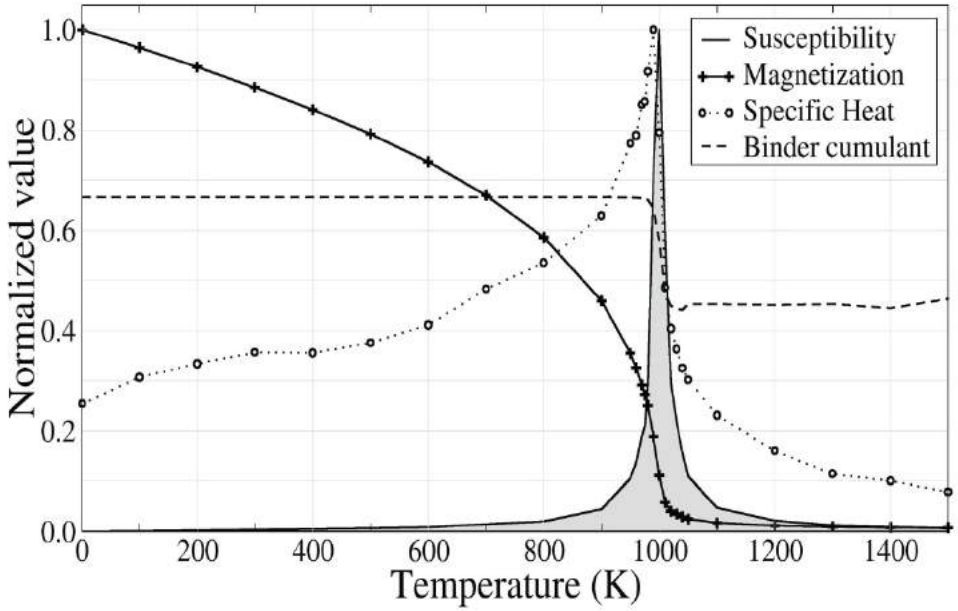

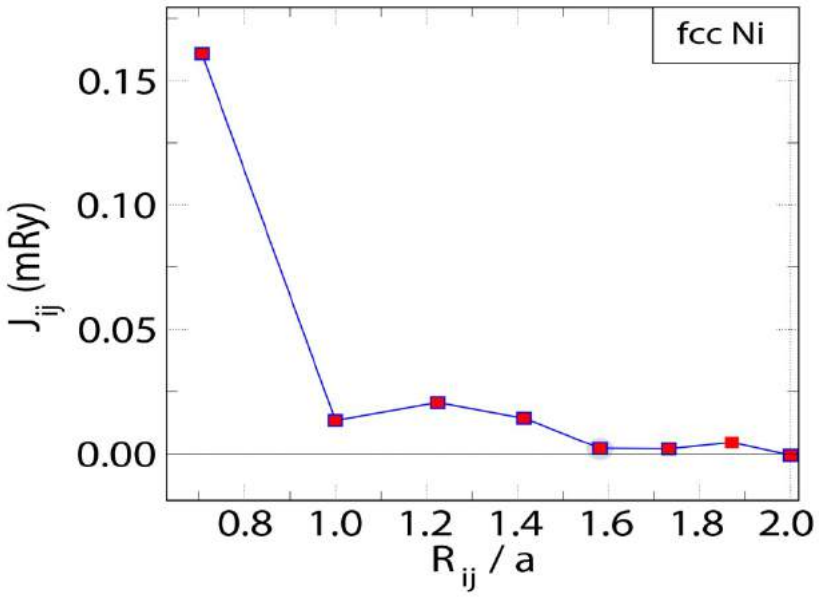

UPPSALA UNIVERSITET

Symmetry resolved interactions

E_g and T_{2g} orbitals in cubic environment

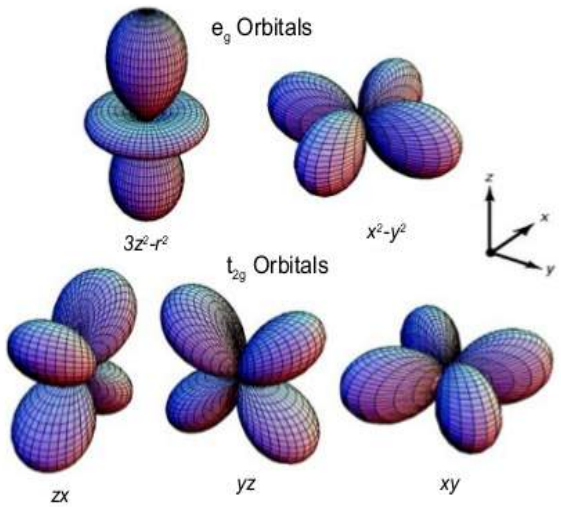

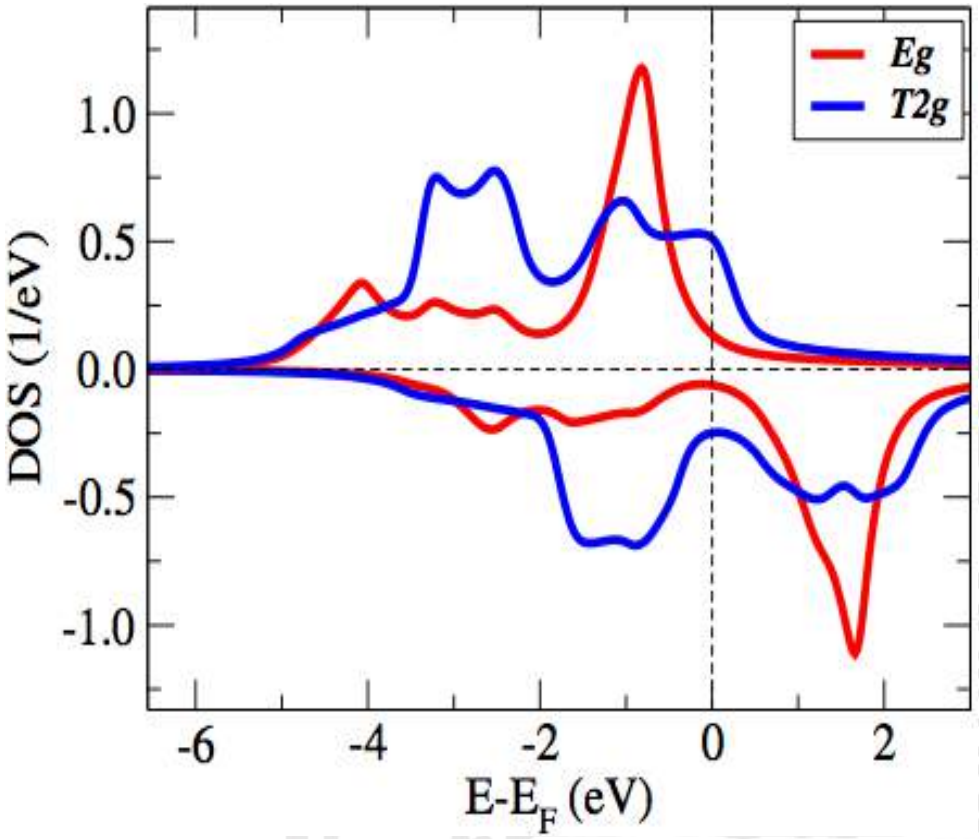

bcc Fe

Interactions along the NN direction — (111)

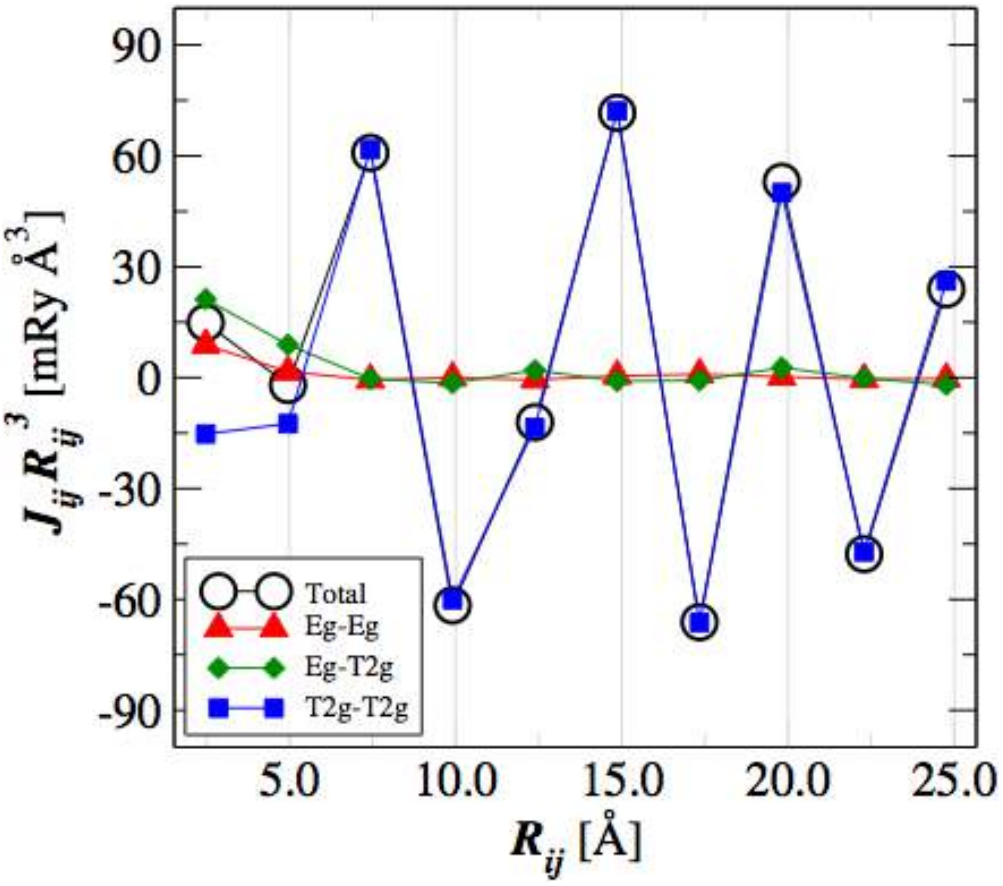

Long-ranged J_{ij}'s are completely defined by T_{2g} states

UPPSALA UNIVERSITET

Atomistic Landau-Lifshitz equation

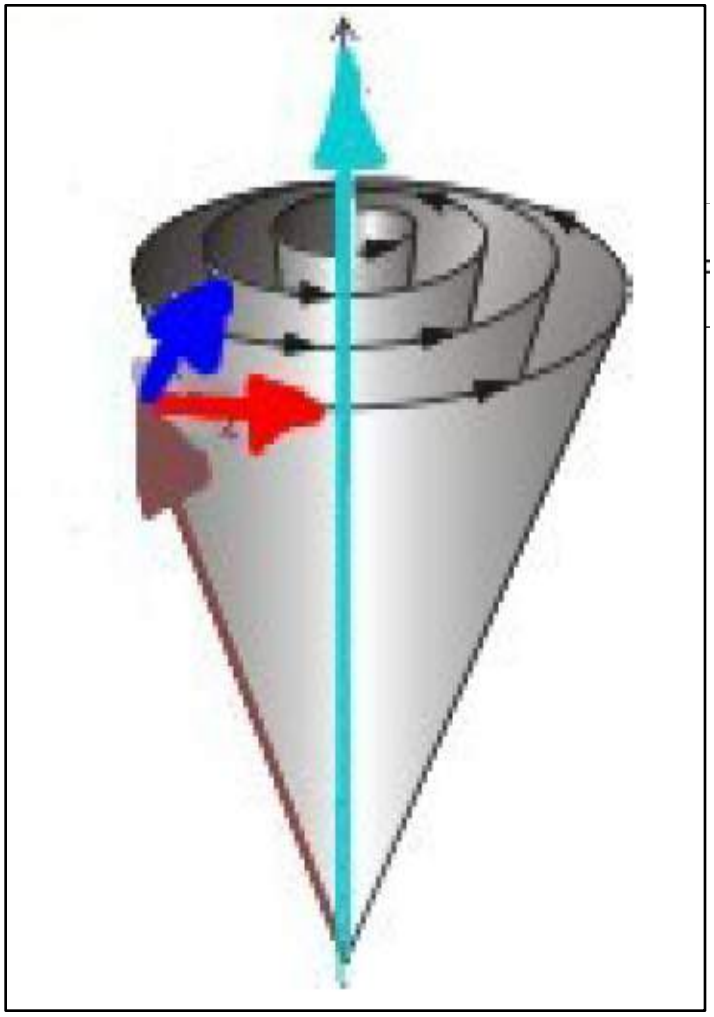

$$\frac{d\mathbf{m_i}}{dt} = -\gamma \mathbf{m_i} \times \mathbf{B_i} - \gamma \frac{\alpha}{m_i} [\mathbf{m_i} \times [\mathbf{m_i} \times \mathbf{B_i}]]$$

Precession Damping

Energy dissipation

$$\frac{dE}{dt} = \frac{dE}{d\mathbf{m}} \cdot \frac{d\mathbf{m}}{dt} = \mathbf{B} \cdot \frac{d\mathbf{m}}{dt}$$

$$\mathbf{B} \cdot \frac{d\mathbf{m}}{dt} \propto 0 + \alpha$$

$$\frac{dE}{dt} \longleftrightarrow \alpha$$

UPPSALA UNIVERSITET

Time scales

Lifetime of magnetic data storage media
http://www.clir.org/pubs/reports/pub54/4life_expectancy.html
http://www.apple.com

Magnetization precession

$$\frac{d\mathbf{m}}{dt} = [\mathbf{m} \times \mathbf{H}] + \frac{\gamma}{m}\left[\mathbf{m} \times \frac{d\mathbf{m}}{dt}\right]$$

$$T \approx 2\pi \frac{m_e}{eB} \approx 36ps \qquad B = 1T$$

Demagnetization by fs Laser
E Beaurepaire et. al, PRL, 76, 4250 (1996)

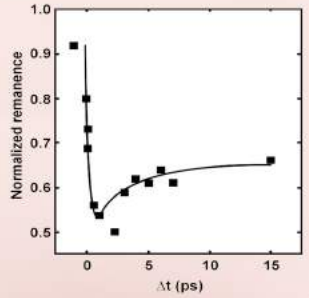

millennium
years
days
s
ms
µs
ns
ps
fs
as
10^{12} 10^{9} 10^{6} 10^{3} 1 10^{-3} 10^{-6} 10^{-9} 10^{-12} 10^{-15} 10^{-18}
t [s]

Geomagnetic reversal
http://en.wikipedia.org/wiki/Earth's_magnetic_field

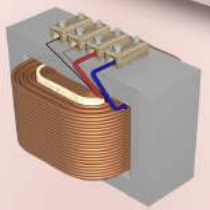

AC Transformer
http://en.wikipedia.org/wiki/Transformer

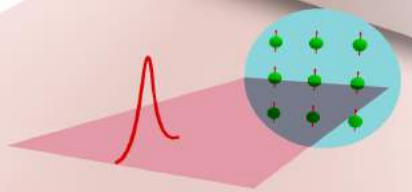

Coherent interaction between light and magnetization
Bigot et. al, Nat Phy vol 5(7), 515 (2009)

UPPSALA UNIVERSITET

Spin wave dispersion spectrum

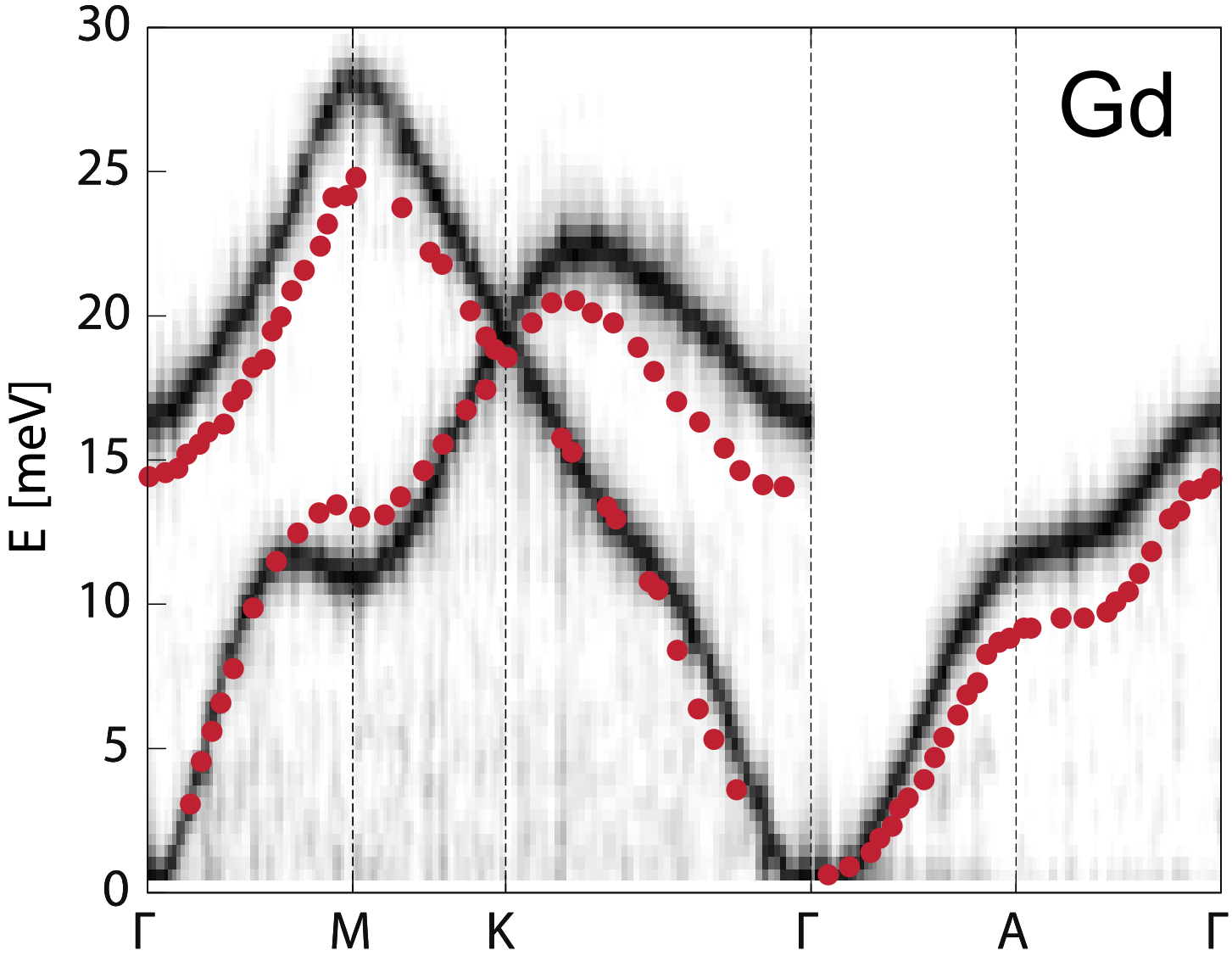

UPPSALA UNIVERSITET

Solitonics

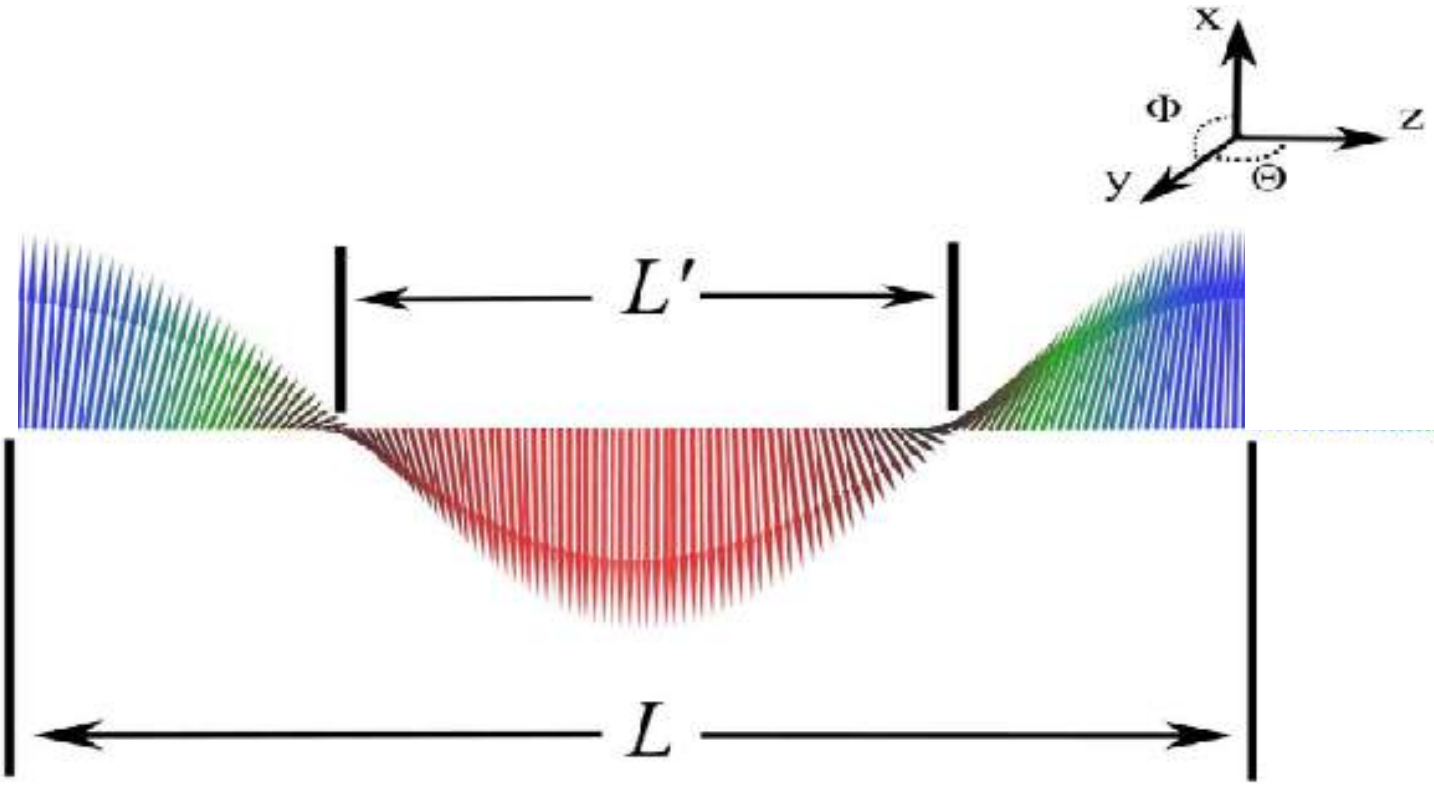

A chiral clot of energy, being the solution to the sine-Gordon equation:

$$\Phi_{tt} - \Phi_{zz} + sin\Phi = 0$$

UPPSALA UNIVERSITET

Magnonics